Arabian Journal of Chemistry (2022) **15**, 103497

King Saud University

Arabian Journal of Chemistry

www.ksu.edu.sa
www.sciencedirect.com

ORIGINAL ARTICLE

Design, synthesis of new novel quinoxalin-2(1*H*)-one derivatives incorporating hydrazone, hydrazine, and pyrazole moieties as antimicrobial potential with *in-silico* ADME and molecular docking simulation

Ahmed Ragab [a,*], Doaa M. Elsisi [b], Ola A. Abu Ali [c], Moustafa S. Abusaif [a], Ahmed A. Askar [d], Awatef A. Farag [b], Yousry A. Ammar [a,*]

[a] *Department of Chemistry, Faculty of Science (Boys), Al-Azhar University, Nasr City 11884, Cairo, Egypt*
[b] *Department of Chemistry, Faculty of Science (Girls), Al-Azhar University, Nasr City, Cairo, Egypt*
[c] *Department of Chemistry, College of Science, Taif University, P.O. Box 11099, Taif 21944, Saudi Arabia*
[d] *Department of Botany and Microbiology, Faculty of Science (Boys), Al-Azhar University, Nasr City, Cairo, Egypt*

Received 29 July 2021; accepted 10 October 2021
Available online 19 October 2021

KEYWORDS

Quinoxaline derivatives,
Antimicrobial activity;
MIC, MBC and MFC;
Multi-drug resistance bacteria (MDRB);
DNA gyrase;
In silico ADME and molecular docking

Abstract A series of 6-(morpholinosulfonyl)quinoxalin-2(1*H*)-one based hydrazone, hydrazine, and pyrazole moieties were designed, synthesized, and evaluated for their *in vitro* antimicrobial activity. All the synthesized quinoxaline derivatives were characterized by IR, NMR (^{1}H /^{13}C), and EI MS. The results displayed good to moderate antimicrobial potential against six bacterial, and two fungal standard strains. Among the tested derivatives, six quinoxalin-2(1*H*)-one derivatives **4a**, **7**, **8a**, **11b**, **13**, and **16** exhibited a significant antibacterial activity with MIC values (0.97–62.5 μg/mL), and MBC values (1.94–88.8 μg/mL) compared with Tetracycline (MICs = 15.62–62.5 μg/mL, and MBCs = 18.74–93.75 μg/mL), and Amphotericin B (MICs = 12.49–88.8 μg/mL, and MFC = 34.62–65.62 μg/mL). In addition, according to CLSI standards, the most active quinoxalin-2(1*H*)-one derivatives demonstrated bactericidal and fungicidal behavior. Moreover, the most active quinoxaline derivatives showed a considerable antibacterial activity with bactericidal potential against multi-drug resistance bacteria (MDRB) strains with MIC values ranged between (1.95–15.62 μg/mL), and MBC values (3.31–31.25 μg/mL) near to standard Norfloxacin

* Corresponding authors.
E-mail addresses: ahmed_ragab@azhar.edu.eg, Ahmed_ragab7@ymail.com (A. Ragab), yossry@azhar.edu.eg, yossry@yahoo.com (Y.A. Ammar).

Peer review under responsibility of King Saud University.

Production and hosting by Elsevier

https://doi.org/10.1016/j.arabjc.2021.103497

(MIC = 0.78–3.13 μg/mL, and MBC = 1.4–5.32 μg/mL. Further, *in vitro S. aureus* DNA gyrase inhibition activity were evaluated for the promising derivatives and displayed potency with IC_{50} values (10.93 ± 1.81–26.18 ± 1.22 μM) compared with Ciprofloxacin (26.31 ± 1.64 μM). Interestingly, these derivatives revealed as good immunomodulatory agents by a percentage ranging between 82.8 ± 0.37 and 142.4 ± 0.98 %. Finally, some *in silico* ADME, toxicity prediction, and molecular docking simulation were performed and showed a promising safety profile with good binding mode.

1. Introduction

Multidrug-resistant bacteria have become a serious concern in many countries around the world in recent decades. The medical community has been seriously affected by the infections caused by these bacteria, and the necessity for treatment has led to research into new antimicrobials agents (Cheesman et al., 2017; Wise et al., 1998). Infections as rheumatic, diarrhea, food poisoning, and salmonellosis are caused by multidrug-resistant gram-negative and gram-positive pathogens such as *S. typhimurium E. coli*, *S. aureus*, and *S. pyogenes* (Ayliffe, 1997; Khan and Asiri, 2011). These infections are responsible for a high mortality rate in both our community and hospitals (Almeida et al., 2021; Mitevska et al., 2021; Wanger and Chávez, 2021). As a result of these parasitic, bacterial infections, millions of people around the subtropical regions are infected, and 20,000 deaths every year. Ciprofloxacin, Amoxicillin, and Norfloxacin are the most commonly used antibiotics for treating bacterial infections since they are effective against intestinal and extra-intestinal wall infections (Guo et al., 2021; Ito and Budke, 2021). However, microbial infections have been increasing dramatically and are currently estimated to affect approximately 1.2 billion people globally (Denning and Bromley, 2015; Zhao et al., 2018).

The incidence of invasive fungal infections (IFIs) and the emergence of resistant fungal pathogens have increased markedly, leading to high morbidity and mortality in immune-compromised patients, such as patients receiving organ transplants, patients undergoing anticancer chemotherapy, and patients with AIDS (Campoy and Adrio, 2017; Liu et al., 2011). Clinically, the three fungal genera, *aspergillus*, *candida*, and *cryptococcus* account for most fungal infections (Denning and Hope, 2010). The common antifungal agents currently used in the clinic are Amphotericin B, Nystatin, Echinocandins, Caspofungin, and Micafungin (Langebrake et al., 2014; Surarit and Shepherd, 1987). As a result, discovering and developing a new class of antimicrobial drugs is critical to fighting the increasing danger of drug-resistant microbes (El-Attar et al., 2018).

Quinoxalines form an attractive biologically active molecule as these are a part of various antibiotics (Kim et al., 2004). The quinoxaline antibiotics of bicyclic showed activity against gram-positive bacteria (Shōji and Katagiri, 1961) and certain animal tumors (Xu et al., 2016) and also are potent inhibitors of RNA synthesis (Khatoon and Abdulmalek, 2021). The mechanism of action occurs by binding to DNA, in which they function as bifunctional intercalating agents. Two antibiotic families of the antibiotic Echinomycin (Kim et al., 2004) and the Triostins are well known. Both series are similar in composition; they consist of two quinoxaline-2-carboxylic acid moieties (Ughetto et al., 1985) (Fig. 1).

Furthermore, marketed drugs, such as Levomycin, Actinoleutin, Quinacillin, contain a quinoxaline ring (Fig. 1) (Bough et al., 1971; Christie et al., 1966; Salwan and Sharma, 2020). Many scientists have reported quinoxalinone derivatives as non-classical analogs of the antifolic agents as Methotrexate and Trimetrexate (Sanna et al., 1998). Additionally, the quinoxaline scaffold is known to be characterized by medically important derivatives with many therapeutical applications as anti-inflammatory (El-Sabbagh et al., 2009), antidiabetic (Yang et al., 2012), anthelmintic (Sakata et al., 1988), antiprotozoal (Guillon et al., 2011), antiviral (Ali et al., 2007), antidepressant (Sarges et al., 1990), antituberculosis (Ancizu et al., 2010), anticancer (Khan et al., 2009), and antimicrobial (Ammar et al., 2020a).

Sulfonamides are well-known antibiotics for treating bacterial infection, malaria, leprosy, etc. (Mondal et al., 2017). In addition, sulfonamides are commonly used antibacterial agents worldwide, owing to their low toxicity, low cost, and excellent efficacy against common bacterial diseases (Özbek et al., 2007). Sulfa drugs exert their bactericidal effect by inhibiting the metabolic pathway of the enzyme dihydropteroate synthetase (DHPS). Folate, a vital agent for forming nucleic acids (DNA, RNA) in the cells, is synthesized by direct participation of DHPS in a catalytic cycle (Epstein et al., 1997; Mondal et al., 2017; Smilack, 1999). Prolonged consumption of sulfonamides shows some adverse reactions to the liver, kidney, skin, lung, heart, and blood (Mondal et al., 2017). These side effects have demanded worldwide effort to search for new generation drugs. The literature reveals that the presence of a morpholine ring on a heterocyclic system contributes to enhanced pharmacological activities in many cases (El-sharief et al., 2019; Muhammad et al., 2017).

Furthermore, the hydrazone function, $R_1R_2C = NR_3–NR_4$ (R = alkyl, aryl or H), is an important pharmacophore in a variety of drugs, especially antibiotic drugs as Thioacetazone, Furazolidone, Nitrofurazone, and Rifampicin (Fig. 1) (Matson and Stupp, 2011). Related hydrazide-hydrazones have been shown to exhibit significant antibacterial (El-Sharief et al., 2016; Hassan et al., 2021), antifungal (Rahman et al., 2005), anticonvulsant (Fayed et al., 2021b; Ragavendran et al., 2007), anticancer (Ammar et al., 2018; Fayed et al., 2020), carbonic anhydrase inhibitors (Wassel et al., 2021b), anti-inflammatory (Salgın-Gökşen et al., 2007), and antimalarial activity (Verma et al., 2014).

Because of the findings mentioned earlier, and as a continuation of our effort in medicinal chemistry (Fayed et al., 2021a; Rizk et al., 2020; Selim et al., 2019; Wassel et al.,

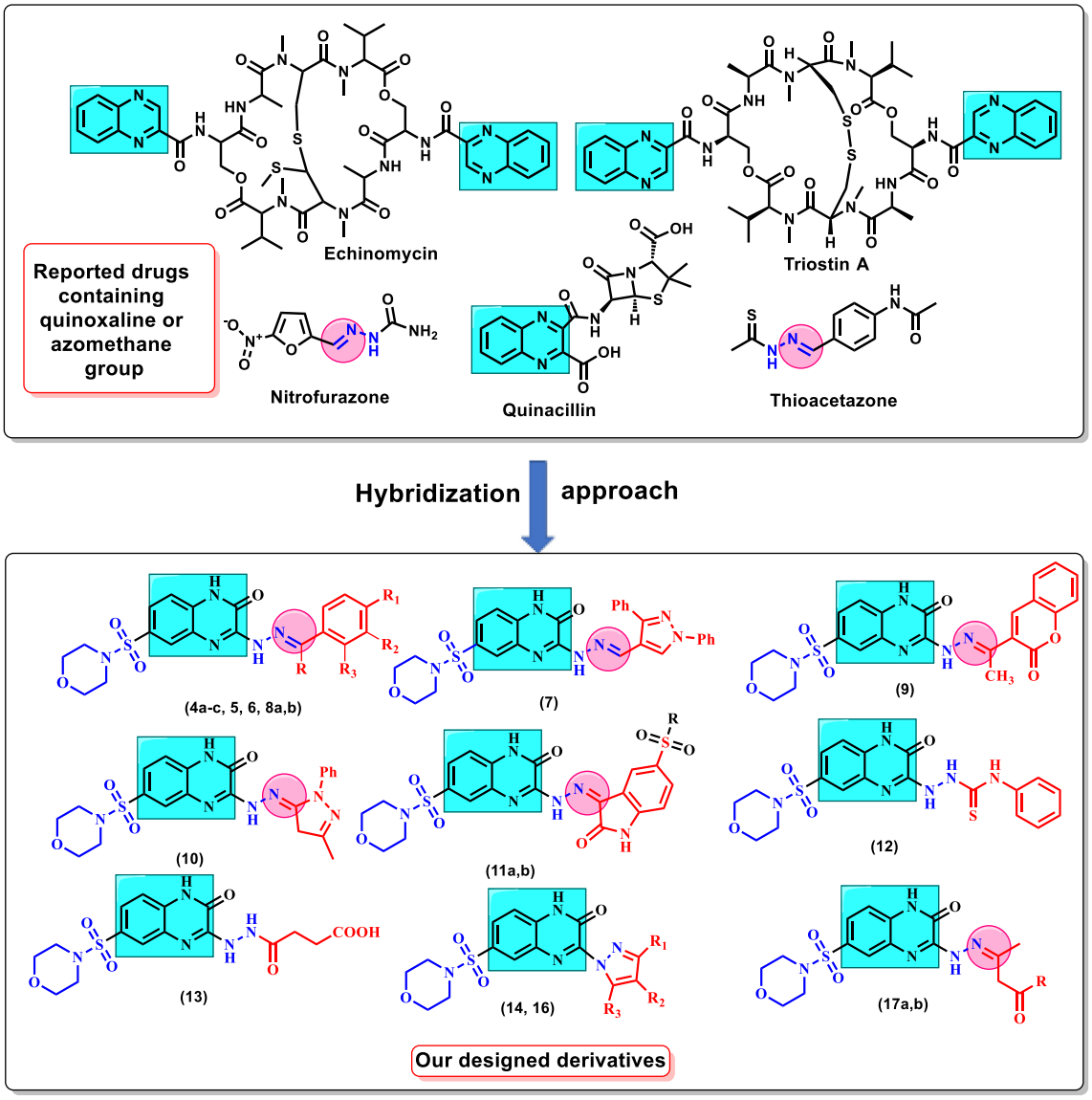

Fig. 1 Rational design of the target quinoxaline derivatives and previously reported quinoxaline or azomethane groups containing drugs.

2021a) and identifying new candidates that may be of value in designing new, potent, selective, and less toxic antibacterial agents (Ibrahim et al., 2021a). We herein reported design, synthesis, and antimicrobial evaluation of novel structure hybrids incorporating the 6-(morpholinosulfonyl)quinoxaline derivatives with hydrazine, hydrazone, and pyrazole. The hybrid of both moieties in a single entity may result in worthwhile molecules with promising antibacterial activity. The antifungal and antibacterial actions of all novel synthetized quinoxaline derivatives were investigated *in vitro* using the agar well diffusion method to determine the inhibition zones (IZs). Besides, the most active quinoxaline derivatives were further evaluated to determine the MIC, MBC/MFC against the standard and multidrug-resistant strains and determine the inhibitory assay of *in vitro S. aerates* DNA gyrase. Besides, the molecular docking simulation inside the active site of DNA gyrase was achieved to determine the binding energy and binding mode. Finally, the *in-silico* prediction of physicochemical, drug-likeness, some pharmacokinetics, medicinal chemistry, and toxicity predictions were calculated using web tools.

2. Material and methods

2.1. Chemistry

With no further purifications, reagents and chemicals were acquired from Aldrich Chemicals, and solvent from Fisher. Melting points (MPs) of all the newly designed compounds were recorded on a digital Gallen Kamp MFB-595 instrument using open capillaries. Within the range of 400–4000 cm^{-1}, IR spectra were calculated using the KBr disc methodology on a Shimadzu 440 spectrophotometer. In NMR spectra (^{1}H / ^{13}C), chemical shifts were calculated in δ/ppm relative

to TMS as an internal default (ppm) that obtained on a JOEL spectrometer 400 / 101 MHz using DMSO d_6 as solvents. The data was provided in the following format: chemical shift, multiplicity (br = broad, m = multiplet, q = quartet, t = triplet, d = doublet, and s = singlet), the coupling constant (J) in Hertz (Hz), and integration. Elemental analysis were carried out at Micro Analytical Unit in Cairo University, Cairo. The mass spectra were calculated at 70 eV using the DI-50 unit of a Shimadzu GC/MSQP5050A Spectrometer at Al-Azhar University's Regional Center for Biotechnology. 6-(Morpholi nosulfonyl)-1,4-dihydroquinoxaline-2,3-dione (**2**) was prepared according to previously reported methods (Ammar et al., 2020a, 2020b).

2.1.1. Synthesis of 3-hydrazinyl-6-(morpholinosulfonyl) quinoxalin-2(1H)-one (3a)

To a solution of dihydroquinoxaline-2,3-dione derivative **2** (1 mmol) in EtOH (5 mL), the hydrazine hydrate (80%) (5 mL) was added dropwise, and the solution was stirred at room temperature for 0.5 hr. Additionally, the reaction mixture was heated under reflux for 3 hs (TLC), then allowed to cool. The solid precipitate that formed was collected by filtration and crystallized from EtOH to yield the desired product.

Yield 81% as yellow crystals; M.p. = 230–232 ℃; IR (KBr, cm^{-1}): 3312, 3245 (NH_2, 2NH), 3025 (CH-Ar.), 2972, 2847 (CH-aliph.), 1678 (C = O), 1621 (C = N) 1332, 1155 (SO_2); ^{1}H NMR (400 MHz, DMSO d_6) δ/ppm 12.19, 9.50 (s, 2H, 2NH; D_2O exchangeable), 7.57 (s, 1H), 7.46 (d, J = 7.6 Hz, 1H), 7.38 (d, J = 8.2 Hz, 1H), 4.79 (s, 2H, NH_2; D_2O exchangeable), 3.62 (t, 4H, $(CH_2)_2O$), 2.88 (t, 4H, $(CH_2)_2N$); ^{13}C NMR (101 MHz, DMSO d_6) δ/ppm 155.23 (C = O), 151.21 (C = C-N), 150.44 (C = N), 135.08, 124.67, 122.98, 117.17, 115.05, 65.76 ($(CH_2)_2O$), 46.35 ($(CH_2)_2N$); MS : (Mwt = 325): m/z, 45.36 (48%), 53.09 (71%), 57.01 (100%), 192.16 (66%), 24.75 (43%), 227.69 (42%), 324 (M^{-1}, 48%), 325.42 (M^+, 49%); Anal. Calcd. for $C_{12}H_{15}N_5O_4S$ (325.34): C, 44.30; H, 4.65; N, 21.53; Found: C, 44.35; H, 4.44; N, 21.41.

2.1.2. Synthesis of hydrazone derivatives linked 6-(morpholinosulfonyl)quinoxalin-2(1H)-one (4–7)

To a solution of 3-(hydrazinyl)quinoxalin-2(1*H*)-one derivative **3a** (1 mmol) in ethanol (25 mL) and various substituted aromatic aldehydes (1 mmol) catalyzed with acetic acid (2 mL). The solution mixture was heated under reflux conditions for a period of 3–6 hs (TLC). The solid precipitate that formed was collected by filtration and crystallized from EtOH/DMF to yield the desired products.

2.1.3. 3-(2-(4-Chlorobenzylidene)hydrazinyl)-6-(morpholinosulfonyl)quinoxalin-2(1H)-one (4a)

Yield 75% as light orange powder; M.p. = 325–327 ℃; IR (KBr, cm^{-1}): 3323, 3228 (2NH), 3067 (CH Ar.), 2946, 2843 (CH aliph.), 1689 (C = O), 1609 (C = N), 1337, 1153 (SO_2); ^{1}H NMR (400 MHz, DMSO d_6) δ/ppm 12.22, 12.02 (s, 2H, 2NH; D_2O exchangeable), 8.70 (s, 1H, CH = N), 7.87 (d, J = 8.4 Hz, 2H), 7.58 (d, J = 8.4 Hz, 2H), 7.47 (s, 1H), 7.42 (dd, J = 8.4, 1.9 Hz, 1H), 7.31 (d, J = 8.4 Hz, 1H), 3.61 (t, 4H, $(CH_2)_2O$), 2.83 (t, 4H, $(CH_2)_2N$); ^{13}C NMR (101 MHz, DMSO d_6): δ /ppm 161.15 (C = O), 155.70 (C = N), 155.33 (CH = N), 133.03, 130.51, 130.28, 129.58, 128.53, 126.60, 122.88, 116.16, 114.95, 65.72 ($(CH_2)_2O$), 46.29 ($(CH_2)_2N$); Anal. Calcd. for $C_{19}H_{18}ClN_5O_4S$ (447.89): C, 50.95; H, 4.05; N, 15.64; Found: C, 50.82; H, 3.88; N, 15.79.

2.1.4. 3-(2-(4-Fluorobenzylidene)hydrazinyl)-6-(morpholinosulfonyl)quinoxalin-2(1H)-one (4b)

Yield 61% as deep orange crystals; M.p. = 335–337 ℃; IR (KBr, cm^{-1}) = 3325, 3210 (2NH), 3068 (CH Ar.), 2955, 2858 (CH aliph.), 1688 (C = O), 1603 (CH = N), 1335, 1152 (SO_2); ^{1}H NMR (400 MHz, DMSO d_6) δ/ppm 12.22, 12.02 (s, 2H, 2NH; D_2O exchangeable), 8.70 (s, 1H, CH = N), 7.91 (d, J = 8.8 Hz, 2H), 7.47 (s, 1H), 7.41 (dd, J = 8.4, 2.0 Hz, 1H), 7.34 (d, J = 8.9 Hz, 2H), 7.28 (d, J = 8.4 Hz, 1H), 3.61 (t, 4H, $(CH_2)_2O$), 2.83 (t, 4H, $(CH_2)_2N$); ^{13}C NMR (101 MHz, DMSO d_6): δ/ppm 160.98 (C = O), 155.71 (C = N), 155.33 (CH = N), 131.21, 131.12, 130.87, 130.84, 128.53, 126.60, 122.87, 116.66, 116.44, 116.16, 114.95, 65.72 ($(CH_2)_2O$), 46.29 ($(CH_2)_2N$); Anal. Calcd. for $C_{19}H_{18}FN_5O_4S$ (431.44): C, 52.89; H, 4.21; N, 16.23; Found: C, 52.98; H, 4.05; N, 16.07

2.1.5. 3-(2-(4-Methoxybenzylidene)hydrzinyl)-6-(morpholinosulfonyl)quinoxalin-2(1H)-one (4c)

Yield 70% as yellow powder; M.p. = 296–298 ℃; IR (KBr, cm^{-1}): 3325, 3296 (2NH), 3057 (CH-Aro.), 2920, 2854 (CH-aliph.), 1677 (C = O), 1608 (CH = N), 1346, 1160 (SO_2); ^{1}H NMR (400 MHz, DMSO d_6) δ/ppm 11.33, 10.68 (s, 2H, 2NH; D_2O exchangeable), 8.61 (s, 1H, CH = N), 8.51 (d, J = 8.4 Hz, 1H), 7.98 (d, J = 8.8 Hz, 1H), 7.78 (d, J = 8.8 Hz, 1H), 7.72 (s, 1H), 7.66 (d, J = 8.8 Hz, 1H), 7.36 (d, J = 8.4 Hz, 1H), 7.02 (d, J = 7.2 Hz, 1H), 3.81 (s, 3H, OCH_3), 3.61 (t, 4H, $(CH_2)_2O$), 2.86 (t, 4H, $(CH_2)_2N$); Anal. Calcd. For $C_{20}H_{21}N_5O_5S$ (443.48): C, 54.17; H, 4.77; N, 15.79; Found: C, 53.92; H, 4.69; N, 15.55.

2.1.6. 3-(2-(2-Hydroxybenzylidene)hydrazineyl)-6-(morpholinosulfonyl)quinoxalin-2(1H)-one (5)

Yield 61% as light yellow powder; M.p. = 318–320 ℃; IR (KBr, cm^{-1}): 3423 (br-OH), 3261 (2NH), 3061 (CH-Aro.), 2973, 2847 (CH-aliph.), 1687 (C = O), 1619 (CH = N), 1339, 1164 (SO_2); ^{1}H NMR (400 MHz, DMSO d_6) δ/ppm 11.91, 11.72, 11.62 (s, 3H, OH; 2NH, D_2O exchangeable), 8.76 (s, 1H, CH = N), 8.74 (s, 1H), 7.61 (d, J = 8.4 Hz, 1H), 7.30 (t, 2H), 6.95 (d, 1H), 6.93 (d, 1H), 6.90 (d, 1H), 3.63 (t, 4H, $(CH_2)_2O$), 2.87 (t, 4H, $(CH_2)_2N$); MS : (Mwt = 429): m/z, 44.05 (40%), 123.92 (87 %), 137.73 (100%), 154.19 (57%), 333.42 (56%), 429.74 (M^+, 13%); Anal. Calcd. For $C_{19}H_{19}N_5O_5S$ (429.45): C, 53.14; H, 4.46; N, 16.31; Found: C, 53.29; H, 4.19; N, 16.15

2.1.7. 3-(2-(4-Hydroxy-3-methoxybenzylidene)hydrazinyl)-6-(morpholinosulfonyl)quinoxalin-2(1H)-one (6)

Yield 63% as pale orange powder; M.p. = 346–348 ℃; IR (KBr, cm^{-1}): 3450 (OH), 3230 (2NH), 3052 (CH-Aro.), 2930, 2845 (CH-aliph.), 1680 (C = O), 1605 (CH = N), 1344, 1163 (SO_2); ^{1}H NMR (400 MHz, DMSO d_6) δ/ppm 11.87, 11.27, 9.53 (s, 3H, OH, 2NH; D_2O exchangeable), 8.47 (s, 1H, CH = N), 8.44 (s, 1H), 7.48 (dd, J = 8.4, 2.0 Hz, 1H), 7.38 (d, J = 8.4 Hz, 1H), 7.29 (s, 1H), 7.08 (dd, J = 8.4, 1.8 Hz, 1H), 6.83 (d, J = 8.0 Hz, 1H), 3.84 (s, 3H, OCH_3), 3.61 (t, 4H, $(CH_2)_2O$), 2.86 (t, 4H, $(CH_2)_2N$); ^{13}C NMR

(101 MHz, DMSO d_6): δ/ppm 158.00 (C = O), 157.87 (C = N), 155.70 (CH = N), 155.33, 151.97, 148.69, 145.11, 131.22, 129.85, 127.83, 125.24, 124.21, 117.43, 116.21, 111.80, 65.73 ($(CH_2)_2O$), 61.80 (OCH_3), 46.35 ($(CH_2)_2N$); Anal. Calcd. For $C_{20}H_{21}N_5O_6S$ (459.48): C, 52.28; H, 4.61; N, 15.24; Found: C, 52.23; H, 4.55; N, 15.19.

2.1.8. 3-(2-((1,3-Diphenyl-1H-pyrazol-4-yl)methylene) hydrazinyl)-6-(morpholinosulfonyl) quinoxalin-2(1H)-one (7)

Yield 77% as deep yellow powder; M.p. = 200–205 ℃; IR (KBr, cm^{-1}): 3356, 3287 (2NH), 3052 (CH-Aro.), 2993, 2913, 2852 (CH-aliph.), 1683 (C = O), 1616 (CH = N), 1360, 1161 (SO_2); ^{1}H NMR (400 MHz, DMSO d_6) δ/ppm 11.52, 9.30 (s, 2H, 2NH; D_2O exchangeable), 9.14 (s, 2H, CH = N, CH-pyrazole), 9.01 (d, J = 8.8 Hz, 1H), 8.83 (d, J = 8.8 Hz, 1H), 8.67 (s, 1H), 8.01 (d, J = 7.6 Hz, 2H), 7.73 (d, J = 6.8 Hz, 2H), 7.49 (t, 3H), 7.36 (t, 3H), 3.63 (t, 4H, $(CH_2)_2O$), 2.87 (t, 4H, $(CH_2)_2N$); ^{13}C NMR (101 MHz, DMSO d_6): δ/ppm 159.66 (C = N), 154.03 (C = O), 153.35 (CH = N), 151.36 (C = N-pyrazole), 148.67, 139.37, 132.24, 131.56, 130.15, 129.33, 129.27, 129.05, 127.74, 127.71, 126.22, 123.78, 120.12, 119.39 , 116.89, 114.77, 66.81 ($(CH_2)_2O$), 42.28 ($(CH_2)_2N$); Anal. Calcd. For $C_{28}H_{25}N_7O_4S$ (555.61): C, 60.53; H, 4.54; N, 17.65; Found: C, 60.50; H, 4.51; N, 17.62.

2.1.9. General method for synthesis of hydrazone derivatives (8–11)

A mixture of 3-(hydrazinyl)quinoxaline derivative **3a** (1 mmol) and substituted ketone derivatives (1 mmol) in EtOH (25 mL), acetic acid as catalyst (2 mL) was added. The solution mixture was heated under reflux for a period of 6–8 hs (TLC), then allowed to cool. The solvent was removed by rotary evaporator and the precipitate was quenched with crushed ice. The resulting precipitate was filtered off, dried and recrystallized from ethanol to yield **(8–11)**.

2.1.10. 3-(2-(1-(4-Bromophenyl)ethylidene)hydrazinyl)-6-(morpholinosulfonyl)quinoxalin-2(1H)-one (8a)

Yield 75% as red powder; M.p. = 183–185℃; IR (KBr, cm^{-1}): 3338, 3224 (2NH), 3071 (CH-Aro.), 2954, 2863 (CH-aliph.), 1691 (C = O), 1609 (C = N), 1337, 1153 (SO_2); ^{1}H NMR (400 MHz, DMSO d_6) δ/ppm 11.72, 10.56 (s, 2H, 2NH; D_2O exchangeable), 8.02 (d, J = 8.4 Hz, 1H), 7.83 (d, J = 8.4 Hz, 1H), 7.34–7.66 (m, 5H), 3.62 (t, 4H, $(CH_2)_2O$), 2.84 (t, 4H, $(CH_2)_2N$), 2.42 (s, 3H, CH_3); ^{13}C NMR (101 MHz, DMSO d_6): δ/ppm 162.13 (C = O), 155.19 (C = N), 142.69, 137.51, 131.64, 129.74, 128.97, 126.90, 126.10, 124.03, 123.11, 115.82, 114.69, 65.74 ($(CH_2)_2O$, 46.32 ($(CH_2)_2N$), 15.14 (CH_3); Anal. Calcd. for $C_{20}H_{20}BrN_5O_4S$ (506.38): C, 47.44; H, 3.98; N, 13.83; Found: C, 47.31; H, 3.75; N, 13.99.

2.1.11. 3-(2-(1-(4-Aminophenyl)ethylidene)hydrazinyl)-6-(morpholinosulfonyl)quinoxalin-2(1H)-one (8b)

Yield 69% as brown crystals; M.p. = > 360 ℃; IR (KBr, cm^{-1}): 3421, 3352, 3278 (NH_2, 2NH), 3089 (CH-Aro.), 2974, 2920, 2858 (CH-aliph.), 1685 (C = O), 1604 (C = N), 1388, 1157 (SO_2); ^{1}H NMR (400 MHz, DMSO d_6) δ/ppm 11.79, 10.29 (s, 2H, 2NH; D_2O exchangeable), 7.92 (s, 1H), 7.83 (d, J = 8.8 Hz, 1H), 7.26 (d, J = 8.4 Hz, 2H), 7.15 (d, J = 8.4 Hz, 2H), 6.58 (d, J = 8.8 Hz, 1H), 5.58 (s, 2H; D_2O exchangeable), 3.61 (t, 4H, $(CH_2)_2O$), 2.84 (t, 4H, $(CH_2)_2N$), 2.36 (s, 3H, CH_3); ^{13}C NMR (101 MHz, DMSO d_6): δ/ppm 164.84 (C = O), 152.22 (C = N), 151.49, 150.82, 136.86, 135.37, 129.25, 128.31, 127.37, 123.79, 123.03, 113.45, 112.90, 111.54, 111.46, 65.75 ($(CH_2)_2O$), 46.33 ($(CH_2)_2N$), 14.65 (CH_3); Anal. Calcd. for $C_{20}H_{22}N_6O_4S$ (442.49): C, 54.29; H, 5.01; N, 18.99; Found: C, 54.11; H, 4.85; N, 19.07

2.1.12. 6-(Morpholinosulfonyl)-3-(2-(1-(2-oxo-2H-chromen-3-yl)ethylidene)hydrazinyl)quinoxalin-2(1H)-one (9)

Yield 71% as deep red crystals; M.p. = 323–325℃; IR (KBr, cm^{-1}): 3356, 3280 (2NH), 3132 (CH-Aro.), 2950, 2857, 2775 (CH-aliph.), 1698 (C = O), 1619 (C = N), 1373, 1154 (SO_2); ^{1}H NMR (400 MHz, DMSO d_6) δ/ppm 11.91, 11.71 (s, 2H, 2NH; D_2O exchangeable), 8.74 (s, 1H), 7.68 (d, J = 8.0 Hz, 1H), 7.54 (dd, J = 8.4, 2.0 Hz, 1H), 7.45 (t, J = 7.6 1H), 7.41 (d, J = 8.4 Hz, 1H), 7.39 (s, 1H), 7.29 (t, 1H), 6.94 (d, J = 8.7 Hz, 1H), 3.62 (t, 4H, $(CH_2)_2O$), 3.31 (s, 3H, CH_3), 2.86 (t, 4H, $(CH_2)_2N$); Anal. Calcd. for $C_{23}H_{21}N_5O_6S$ (495.51): C, 55.75; H, 4.27; N, 14.13; Found: C, 55.71; H, 4.25; N, 14.10.

2.1.13. 3-(2-(5-Methyl-2-phenyl-2,4-dihydro-3H-pyrazol-3-ylidene)hydrazinyl)-6-(morpholino-sulfonyl)quinoxalin-2(1H)-one (10)

Yield 65% as pale brown crystals; M.p. = 310–312 ℃; IR (KBr, cm^{-1}): 3315, 3219 (2NH), 3073 (CH Ar.), 2954, 2851 (CH aliph.), 1690 (C = O), 1608 (C = N), 1336, 1152 (SO_2); ^{1}H NMR (400 MHz, DMSO d_6) δ/ppm 12.08, 12.27 (s, 2H, 2NH; D_2O exchangeable), 8.69 (s, 1H), 8.03 (d, J = 7.6 Hz, 1H), 7.76 (d, J = 7.6 Hz, 1H), 7.26 – 7.59 (m, 5H), 4.35 (s, 2H, CH_2), 3.64 (t, 4H, $(CH_2)_2O$), 2.85 (t, 4H, $(CH_2)_2N$), 2.51 (s, 3H, CH_3); Anal. Calcd. for $C_{22}H_{23}N_7O_4S$ (481.53): C, 54.88; H, 4.81; N, 20.36; Found: C, 54.63; H, 4.97; N, 20.21.

2.1.14. 6-(Morpholinosulfonyl)-3-(2-(5-(morpholinosulfonyl)-2-oxoindolin-3-ylidene)hydrazinyl)-quinoxalin-2(1H)-one (11a)

Yield 84% as reddish orange powder; M.p. = 273–275℃; IR (KBr, cm^{-1}): 3345, 3183 (3NH), 3056 (CH-Aro.), 2963, 2853 (CH-aliph.), 1697 (2C = O), 1614 (C = N), 1335, 1157 (SO_2); ^{1}H NMR (400 MHz, DMSO d_6) δ/ppm 12.03, 11.80, 11.23 (s, 3H, 3NH; D_2O exchangeable), 8.85 (s, 1H), 7.80 (d, J = 8.4 Hz, 1H), 7.71 (d, J = 8.0 Hz, 1H), 7.47 (s, 1H), 7.40 (d, J = 8.4 Hz, 1H), 7.10 (d, J = 8.4 Hz, 1H), 3.63 (t, 8H, $2(CH_2)_2O$), 2.93 (t, 4H, (CH_2)-N), 2.87 (t, 4H, (CH_2)-N); ^{13}C NMR (101 MHz, DMSO d_6) δ/ppm 172.53 (C = O), 163.54 (C = O), 155.70 (C = N), 155.32 (C = C), 151.48, 135.60, 130.28, 128.57, 128.33, 126.60, 122.87, 121.23, 116.16, 114.95, 112.07, 110.73, 65.73 $(CH_2)_2O$), 46.42 $(CH_2)_2N$), MS : (Mwt = 603): m/z, 128.47 (40%), 257.98 (77%), 301.50 (100%), 559.11 (58%), 603.45 (M^+, 13%); Anal. Calcd. for $C_{24}H_{25}N_7O_8S_2$ (603.63): C, 47.76; H, 4.17; N, 16.24; Found: C, 47.93; H, 4.32; N, 16.10.

2.1.15. 6-(Morpholinosulfonyl)-3-(2-(2-oxo-5-(piperidin-1-ylsulfonyl)indolin-3-ylidene)hydrazinyl)-quinoxalin-2(1H)-one (11b)

Yield 82% as orange crystals; M.p. = 288–290 ℃; IR (KBr, cm^{-1}):3365, 3193 (3NH), 3053 (CH-Aro.), 2970, 2850 (CH-

aliph.), 1699 (br-2C = O), 1620 (C = N), 1346, 1152 (SO_2); ^{1}H NMR (400 MHz, DMSO d_6) δ/ppm 12.24, 12.03, 11.19 (s, 3H, 3NH; D_2O exchangeable), 8.82 (s, 1H), 7.79 (d, J = 8.4 Hz, 1H), 7.71 (d, J = 8.0 Hz, 1H), 7.47 (s, 1H), 7.42 (d, J = 8.4 Hz, 1H), 7.05 (d, J = 8.0 Hz, 1H), 3.62 (t, 4H, $(CH_2)_2$-O), 2.92 (t, 4H, $(CH_2)_2$-N), 2.86 (t, 4H, $2CH_2$-pip), 1.53 (m, 4H, $2CH_2$-pip), 1.35 (t, 2H, CH_2-pip); ^{13}C NMR (101 MHz, DMSO d_6) δ/ppm 163.14 (C = O), 155.71 (C = O), 155.33 (C = N), 142.16, 130.30, 128.57, 127.14, 126.62, 124.86, 123.21, 122.87, 116.51, 116.17, 114.96, 110.64, 65.73 ($(CH_2)_2O$), 47.10 ($(CH_2)_2N$), 46.29 ($(CH_2)_2N$), 25.14 ($2CH_2$-pip), 23.31 (CH_2-pip); Anal. Calcd. for $C_{25}H_{27}N_7O_7S_2$ (601.65): C, 49.91; H, 4.52; N, 16.30; Found: C, 49.85; H, 4.49; N, 16.27.

2.1.16. Synthesis of 2-(7-(morpholinosulfonyl)-3-oxo-3,4-dihydroquinoxalin-2-yl)-N-phenyl-hydrazine-1-carbothioamide (12)

To a solution of 3-(hydrazinyl)quinoxaline derivative **3a** (1 mmol), phenyl isothiocyanate (1 mmol) in absolute ethanol (25 mL) with three drops of triethyl amine (TEA) was heated under reflux for 6 hs (TLC). The solid precipitate that formed was collected by filtration and crystallized from EtOH to yield the desired product.

Yield 51% as yellow powder; M.p. = 218–220 ℃; IR (KBr, cm^{-1}): 3201, 3121 (4NH), 3055 (CH– Aro.), 2985, 2972, 2902 (CH-aliph.), 1688 (C = O), 1600 (C = N), 1347, 1159 (SO_2); ^{1}H NMR (400 MHz, DMSO d_6) δ/ppm 12.25, 12.05, 9.52, 9.35 (s, 4H, 4NH; D_2O exchangeable), 8.32 (d, J = 9.1 Hz, 1H), 7.75 (s, 1H), 7.55 (t, 1H), 7.50 (d, 1H), 7.43 (d, 2H), 7.26 (t, 2H), 3.64 (t, 4H, $(CH_2)_2O$), 2.86 (t, 4H, $(CH_2)_2N$); MS: (Mwt = 460): m/z, 63.36 (43%), 74.02 (100%), 413.74 (58%), 454.93 (20 %), 460.23 (M^+, 20%); Anal. Calcd. for $C_{19}H_{20}N_6O_4S_2$ (460.53): C, 49.55; H, 4.38; N, 18.25; Found: C, 49.31; H, 4.54; N, 18.10.

2.1.17. Synthesis of 4-(2-(7-(morpholinosulfonyl)-3-oxo-3,4-dihydroquinoxalin-2-yl)hydrazinyl)-4-oxobutanoic acid (13)

An equimolar mixture of 3-(hydrazinyl)quinoxaline derivative **3a** (1 mmol), and succinic anhydride (1 mmol) in absolute ethanol (25 mL), firstly the reaction mixture was heated under reflux for a period 5 hs (TLC). The resulting mixture was precipitated on hot, collected by filtration, dried and washed with hot ethanol or recrystallized from ethanol/DMF to give the desired product.

Yield 72% as yellow crystals; M.p. = 303–305 ℃; IR (KBr, cm^{-1}): 3350, 3207 (3NH), 3050 (CH Ar.), 2967, 2860 (CH aliph.), 1684 (C = O), 1601 (C = N), 1347, 1154 (SO_2); ^{1}H NMR (400 MHz, DMSO d_6) δ/ppm 12.27, 12.09, 9.74, 8.96 (s, 4H, OH, 3NH; D_2O exchangeable), 7.49 (s, 1H), 7.43 (d, J = 8.4 Hz, 1H), 7.31 (d, J = 8.4 Hz, 1H), 3.67 (t, 4H, $(CH_2)_2O$), 2.86 (t, 4H, $(CH_2)_2N$), 2.44 (t, 2H, CH_2), 2.34 (t, 2H, CH_2); ^{13}C NMR (101 MHz, DMSO d_6) δ/ppm 174.06 (C-OH), 170.38, 155.69 (2C = O), 155.32 (C = N), 130.29, 128.57, 126.61, 122.88, 116.16, 114.95, 65.73 ($(CH_2)_2O$), 46.29 ($(CH_2)_2N$), 29.24 (CH_2), 28.42 (CH_2); MS: (Mwt = 425): m/z, 79.33 (69%), 168.77 (73%), 218.28 (90%), 259.62 (100%), 330.04 (78%), 425.66 (M^+, 58%); Anal. Calcd. for $C_{16}H_{19}N_5O_7S$ (425.42): C, 45.17; H, 4.50; N, 16.46; Found: C, 45.32; H, 4.74; N, 16.23.

2.1.18. Synthesis of ethyl 5-amino-3-(methylthio)-1-(6-(morpholinosulfonyl)-2-oxo-1,2-dihydroqui-noxalin-3-yl)-1H-pyrazole-4-carboxylate (14)

To equimolar amount of 3-(hydrazinyl)quinoxaline derivative **3a** (1 mmol) and ethyl 2-cyano-3,3-bis(methylthio)acrylate (1 mmol) in absolute ethanol (25 mL) was heated under reflux for 5 hs (TLC). The solid precipitate that formed was collected by filtration and crystallized from EtOH/DMF to yield the desired product (**14**).

Yield 68% as light yellow crystals; M.p. = 283–285 ℃; IR (KBr, cm^{-1}): 3410, 3350, 3260 (NH_2, NH), 3034 (CH-Aro.), 2904, 2825 (CH-aliph.), 1690 (C = O), 1615 (C = N), 1357, 1162 (SO_2); ^{1}H NMR (400 MHz, DMSO d_6) δ/ppm 13.16 (s, 1H, NH; D_2O exchangeable), 8.12 (s, 1H), 7.87 (d, J = 8.8 Hz, 1H), 7.60 (d, J = 8.4 Hz, 1H), 6.92 (s, 2H, NH_2, D_2O exchangeable), 4.23 (q, 2H, CH_2), 3.62 (t, 4H, $(CH_2)_2O$), 2.91 (t, 4H, $(CH_2)_2N$), 2.36 (s, 3H, S-$\underline{CH_3}$), 1.27 (t, 3H, ($\underline{CH_3}$-CH_2)); MS: (Mwt = 496): m/z, 82.42 (44%), 137.38 (100 %), 197.56 (44%), 357.35 (53%), 421.79 (57%), 459.09 (69%), 472.08 (51%), 494.96 (M^{+1}, 15%); Anal. Calcd. for $C_{19}H_{22}N_6O_6S_2$ (494.54): C, 46.15; H, 4.48; N, 16.99; Found: C, 46.43; H, 4.31; N, 16.84.

2.1.19. Synthesis of 5-amino-3-(cyanomethyl)-1-(7-(morpholinosulfonyl)-3-oxo-3,4-dihydroquinoxalin-2-yl)-1H-pyrazole-4-carbonitrile (16)

An equimolar amount of 3-(hydrazinyl)quinoxaline derivative **3a** (1 mmol) and 2-amino-1,1,3-propenetricarbonitrile (1 mmol) in absolute ethanol (25 mL). The reaction mixture was allowed to cool after being heated under reflux for 8 hs (TLC). The solid precipitate that formed was collected by filtration and crystallized from EtOH to yield the desired product.

Yield 60% as light red crystals; M.p. = 200–202 ℃; IR (KBr, cm^{-1}): 3307, 3203 (NH_2, NH), 3060 (CH-Aro.), 2971, 2902, 2860 (CH-aliph.), 2286 (CH_2-$\underline{C{\equiv}N}$), 2204 (C≡N), 1684 (C = O), 1608 (C = N), 1343, 1156 (SO_2); ^{1}H NMR (400 MHz, DMSO d_6) δ/ppm 9.27 (s, 1H, NH; D_2O exchangeable), 7.60 (s, 1H), 7.50 (s, 2H, NH_2; D_2O exchangeable), 7.43 (d, J = 8.0 Hz, 1H), 7.31 (d, J = 8.4 Hz, 1H), 3.63 (t, 4H, $(CH_2)_2O$), 3.17 (s, 2H, $\underline{CH_2}$-C≡N), 2.86 (t, 4H, $(CH_2)_2N$); MS: (Mwt = 440): m/z, 50.33 (45%), 65.43 (100%), 103.95 (53%), 234.40 (55%), 267.49 (51%), 440.00 (M^+, 7%); Anal. Calcd. for $C_{18}H_{16}N_8O_4S$ (440.44): C, 49.09; H, 3.66; N, 25.44; Found: C, 48.92; H, 3.83; N, 25.29.

2.1.20. General method for synthesis of hydrazone derivatives (17a, b)

An equimolar amount of 3-(hydrazinyl)quinoxaline derivative **3a** (1 mmol) and requisite active methylene (ethyl acetoacetate or acetyl acetone) (1 mmol) in absolute ethanol (25 mL). The suspension was heated under reflux for a period 5–7 hs (TLC), then allowed to cool. The precipitate that formed was collected by filtration and crystallized from EtOH/ DMF to afford the desired product.

2.1.21. Ethyl-3-(2-(7-(morpholinosulfonyl)-3-oxo-3,4-dihydroquinoxalin-2-yl)hydrazineylidene) Butanoate (17a)

Yield 58% as yellowish crystals; M.p. = 205–208 ℃; IR (KBr, cm^{-1}): 3354, 3244 (2NH), 3065 (CH Ar.), 2970, 2901, 2862

(CH-aliph.), 1684 (br 2C = O), 1609 (C = N), 1347, 1160 (SO_2); ^{1}H NMR (400 MHz, DMSO d_6) δ/ppm 12.18 (br s, 2H, 2NH; D_2O exchangeable), 7.49 (s, 1H), 7.43 (d, J = 8.4 Hz, 1H), 7.31 (d, J = 8.4 Hz, 1H), 4.13 (q, 2H, (CH_3-$\underline{CH_2}$)), 3.64 (t, 4H, $(CH_2)_2O$), 3.58 (s, 2H, CH_2), 3.17 (s, 2H, $\underline{CH_2}$.C≡N), 2.89 (t, 4H, $(CH_2)_2N$), 2.18 (s, 3H, CH_3), 1.21 (t, 3H, ($\underline{CH_3}$-CH_2)); ^{13}C NMR (101 MHz, DMSO d_6) δ/ppm 155.71 (C = O), 155.33 (C = N), 153.58 (C = O), 130.74, 130.30, 128.51, 126.62, 122.88, 116.16, 114.94, 65.72 ($(CH_2)_2O$), 60.94 (CH_3-$\underline{C}H_2$), 50.05 (CH_2), 46.29 ($(CH_2)_2N$), 30.55 (CH_3), 14.54 ($\underline{C}H_3$-CH_2); MS: (Mwt = 437): m/z, 70.28 (84%), 119.37 (42%), 158.09 (44 %), 298.54 (42%), 352.95 (100%), 369.41 (77%), 437.07 (M^+, 16%); Anal. Calcd. for $C_{18}H_{23}N_5O_6S$ (437.47): C, 49.42; H, 5.30; N, 16.01; Found: C, 49.59; H, 5.15; N, 15.86.

2.1.22. 6-(Morpholinosulfonyl)-3-(2-(4-oxopentan-2-ylidene) hydrazinyl)quinoxalin-2(1H)-one (17b)

Yield 62% as red crystals; M.p. = 310–312°C; IR (KBr, cm^{-1}): 3362, 3220 (2NH), 3054 (CH-Aro.), 2947, 2866 (CH aliph.), 1687 (br 2C = O), 1622 (C = N), 1335, 1164 (SO_2); ^{1}H NMR (400 MHz, DMSO d_6) δ/ppm 12.22, 12.04 (s, 2H, 2NH; D_2O exchangeable), 7.47 (s, 1H), 7.41 (d, J = 8.4 Hz, 1H), 7.28 (d, J = 8.4 Hz, 1H), 3.99 (s, 2H, CH_2), 3.61 (t, 4H, $(CH_2)_2O$), 2.83 (t, 4H, $(CH_2)_2N$), 2.10 (s, 3H, CO$\underline{CH_3}$), 1.89 (s, 3H, CH_3); MS: (Mwt = 407): m/z, 53.49 (100%), 76.18 (50 %), 94.18 (65%), 215.21 (40%), 353.52 (32%), 407.45 (M^+, 4%); Anal. Calcd. for $C_{17}H_{21}N_5O_5S$ (407.45): C, 50.11; H, 5.20; N, 17.19; Found: C, 50.02; H, 5.03; N, 17.36

2.2. Biological activity (all details in supplementary material file)

The antimicrobial activity of the newly designed derivatives were evaluated against three gram-negative strains, namely (*E. coli* ATCC 25922, *P. aeruginosa* ATCC 27853, and *S. typhi* ATCC 6539) , three gram-positive strains (*B. subtilis* ATCC 6633, *S. aureus* ATCC 29213, and *E. faecalis* ATCC 29212), and two fungal strains as (*C. albicans* ATCC 10231, and *F. oxysporum* RCMB 008002). The inhibition zone represented as the diameter of the inhibition zones by mm were evaluated by the agar well diffusion method according to previously reported methods (A Ammar et al., 2016; Ammar et al., 2017).

For the most promising derivatives **4a**, **7**, **8a**, **11b**, **13**, and **16** depending on the zone of inhibition, the minimal inhibitory concentration were performed and verified using the broth micro-dilution procedure outlined in the (CLSI) Laboratory Standards Institute guidelines (Wikler et al., 2008). Both Tetracycline and Amphotericin B were used as positive controls.

Additionally, the most active derivatives **4a**, **7**, **8a**, **11b**, **13**, and **16** were screened and determine both MIC and MBC against multidrug resistance strains as gram-negative, namely (*P. aeruginosa* ATCC BAA-2111, and *E. coli ATCC BAA*-196), and gram-positive (*S. aureus* ATCC 43300, and *S. aureus* ATCC 33591) according to previously reported methods (Ammar et al., 2021; Ragab et al., 2021). Tetracycline, as well as Norfloxacin, were evaluated as positive controls.

The immunomodulatory activity using nitro-blue tetrazolium (NBT) reduction (R.L. Baehner, 1968) and *in-vitro* DNA gyrase inhibitory assay for the most active derivatives **4a**, **7**, **8a**, **11b**, **13**, and **16** were evaluated according to our previous work (Alt et al., 2011).

2.3. Molecular docking study

The molecular docking study was performed inside the active site of *S. aerates* DNA gyrase (PDB: 2XCT) using the Molecular Operating Environmental (MOE) 10.2008 according to the previously reported methods (Ibrahim et al., 2021b; Ragab et al., 2021).

3. Results and discussion

3.1. Chemistry

The target quinoxaline derivatives were synthesized using the synthetic approaches depicted in Schemes 1-3. The starting material 3-hydrazino-7-(morpholinosulfonyl)-3,4-dihydroqui noxalin-2(1*H*)-one (**3a**) in a good yield was synthesized *via* interaction of 2,3-dioxo-1,2,3,4-tetrahydroquinoxaline-6-sulfo nyl chloride (**1**) with one mole of morpholine to yield the 6-(morphilonosulfonyl)-2,3-dioxoquinoxaline derivative **2** according to the reported method (Ammar et al., 2020b). The 6-(morpholinosulfonyl)quinoxaline derivative **2** underwent hydrazinolysis with an equivalent amount of hydrazine to get a sole product conceived as 3-hydrazine-6-morpholino sulfonylquinoxaline (**3a)** or 2-hydrazine-6-morpholinosulfo nyl-quinoxaline (**3b)**. Based on the electron-withdrawing property of the sulfonyl group and according to the theoretical calculation of energy (**see supplementary material results for DFT calculation**) and according to reported method (Elsisi et al., 2022), the isomer **3a** structure is more favorable, and the reactions will be completed on the 3-carbon center *via* a nucleophilic substitution mechanism. The IR analysis of 3-(hydrazinyl)quinoxaline derivative **3a** demonstrated absorption bands at υ 3312, 3245, 1678, and 1332, 1155 cm^{-1} characteristic for NH_2, NH, C = O, and SO_2 groups. Additionally, the ^{1}H NMR spectrum showed three exchangeable signals at δ 12.19, 9.50, and 4.79 ppm corresponding to the protons of two NH and NH_2, as well as two triplet signals at δ 3.62 and 2.88 ppm characteristic for the morpholinyl group protons ($(CH_2)_2O$) and $(CH_2)_2N$), respectively. Besides, the aromatic protons that appeared between δ 7.38–7.57 ppm. Moreover, the ^{13}C NMR data of compound **3a** revealed signals at δ 65.76, 46.35 ppm characteristic for the morpholine carbons ($(CH_2)_2O$) and $(CH_2)_2N$), respectively, as well as three signals at δ 155.23, 151.21, and 150.44 characteristics for carbonyl, C = $\underline{C}$-N, and C = N groups, respectively. Also, the signals of aromatic carbons appeared in the range of δ 115.05–135.08 ppm. The mass spectrum demonstrated molecular ion peak at m/z = 325 and base peak at m/z = 57, which agrees with its calculated molecular formula $C_{12}H_{15}N_5O_4S$.

Thus, refluxing of 3-(hydrazinyl)quinoxaline derivative **3a** with formyl derivatives afforded the corresponding hydrazone derivatives **4**–**7**. The elemental analysis and spectral data were used to elucidate the structure of the synthesized compounds. The IR spectra of hydrazono-quinoxaline derivative **4b** demonstrated absorption bands at υ 3323, 3210, 1688 cm^{-1} characteristic for NH and carbonyl groups. The ^{1}H NMR spectrum of hydrazono-quinoxaline derivative **4b** showed

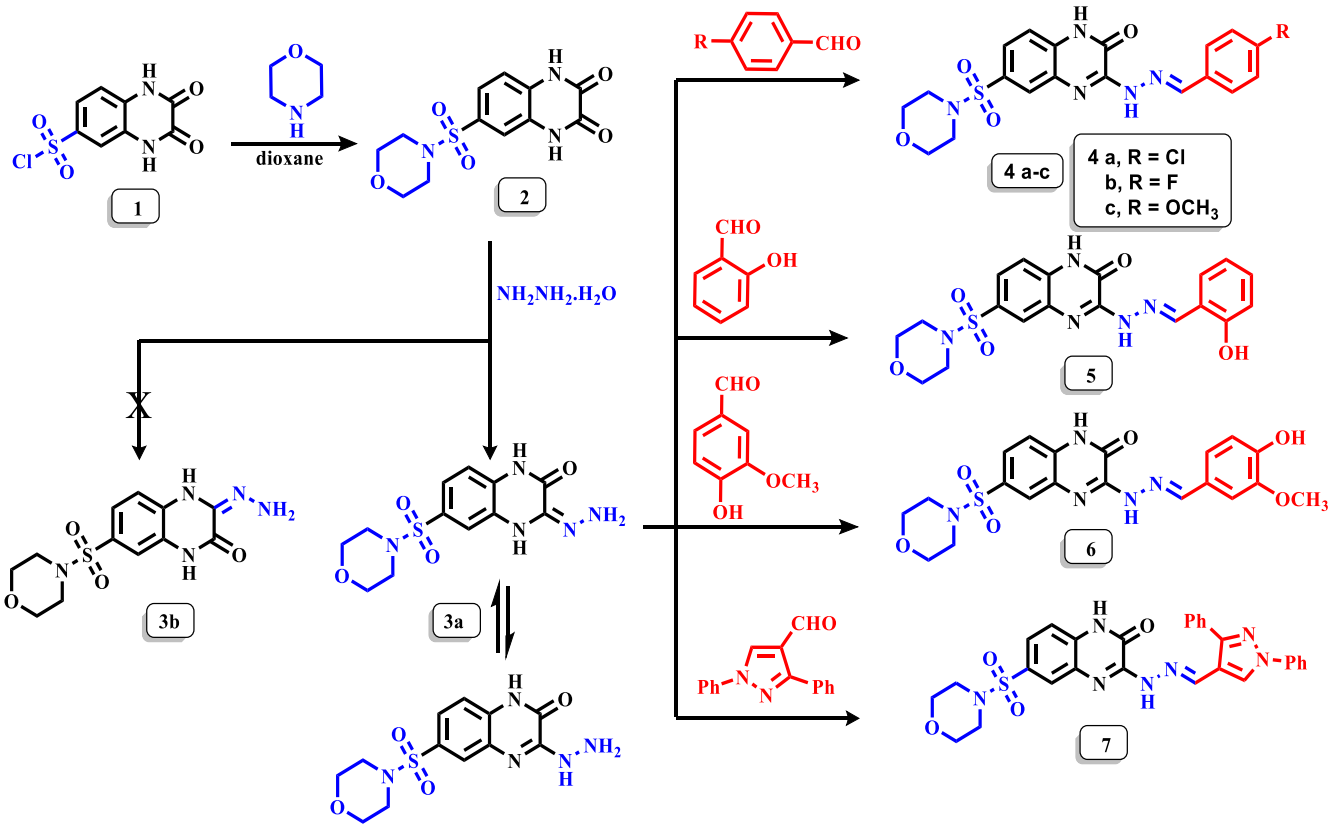

Scheme 1 Synthesis of new Schiff base derivative **4a-c, 5, 6,** and **7** incorporating quinoxaline pharmacophore moiety.

two triplet signals at δ 2.83, 3.61 ppm for the morpholine protons ($(CH_2)_2N$) and ($(CH_2)_2O$) respectively, one singlet signal at δ 8.70 ppm for methine-H, and two exchangeable singlet signals at δ 12.02 and 12.22 ppm referred to the protons of two NH groups. ^{13}C NMR spectra showed two signals at δ 46.29, 65.72 for morpholine carbons, aromatic carbons in the range of δ 114.95–131.21 ppm and three signals at δ 155.33, 155.71 and 160.98 ppm for CH = N, C = N and C = O carbons, respectively. Besides, the elemental analysis and spectroscopic data were used to elucidate the structure of hydrazone derivative **4b**. Additionally, the IR spectra of hydrazine derivative **6** demonstrated absorption bands at υ 3450, 3230, 1680, and 1605 cm^{-1} characteristic for OH, NH, C = O, and C = N groups, respectively. Furthermore, the ^{1}H NMR spectrum showed a significant signal at δ 3.84 ppm characteristic for methoxy group, and three exchangeable singlet signals at δ 11.87, 11.27, and 9.53 ppm characteristic for two NH and OH protons. Moreover, the ^{13}C NMR spectra showed signals at δ 61.80 ppm characteristic for methoxy group, three signals at δ 158.00, 157.87 and 151.70 ppm related for C = O and two C = N groups, respectively, besides the signals of aromatic carbons ranged between δ 111.80–155.70 ppm (Scheme 1).

Moreover, condensation of 3-(hydrazinyl)quinoxaline derivative **3a** with some acetyl derivatives afforded the corresponding 2-(1-(substituted-aryl)ethylidene)hydrazono-quinoxaline derivatives (**8, 9**). IR spectra of hydrazine derivative **8a** demonstrated stretching vibration bands at υ 3224, 1691, and 1609 cm^{-1} characteristic for NH, C = O, and C = N groups, respectively. Also, its ^{1}H NMR spectrum revealed a new signal owning to the methyl protons at δ 2.42 ppm and two exchangeable signals related to two NH protons at δ 10.56 and 11.72 ppm. Besides, signals are characteristic of morpholine and aromatic protons. Its ^{13}C NMR spectra revealed the signal for the methyl group at δ 15.14 ppm, two signals at δ 155.19, and 162.13 ppm for carbonyl (C = O), and C = N, besides signals between δ 114.69–142.69 ppm related to the aromatic carbons.

Similarly, the hydrazide derivative was subjected to react with some selected keto heterocyclic compounds such as pyrazolone and isatin derivatives where hydrazone-quinoxaline derivatives **10**, **11** were obtained. For the spectroscopic analysis of previous hydrazone templates, compound **11b** was used as an example. Its IR spectrum showed characteristic stretching vibrational frequencies for N–H, C = O, and C = N at υ 3228, 3193, 1699, and 1612 cm^{-1}, respectively. Moreover, the ^{1}H NMR of compound **11b** showed three singlet signals corresponding to three N–H at δ 11.19, 12.03, and 12.24 ppm that are exchangeable with D_2O. Besides, three triplet signals and two multiplets were observed at δ 3.62, 2.92, 2.86, 1.53, and 1.35 ppm, characteristic of the morpholinyl and piperidinyl protons. Further, the ^{13}C NMR revealed signals at δ 23.31, 25.14, 46.29, 47.10, and 65.73 ppm due to the piperidinyl and morpholinyl carbons, in addition to the aromatic carbons that ranged between δ 110.64–142.16 ppm and two carbonyl groups at δ 155.71, 163.14 ppm (Scheme 2).

The thiosemicarbazide derivative **12** was obtained upon treatment of the 3-(hydrazinyl)quinoxaline derivative **3a** with phenyl isothiocyanate. The ^{1}H NMR spectrum of thiosemicarbazide derivative **12** led to the appearance of four singlet signals at δ 9.35, 9.52, 12.05, 12.25 ppm for four NH protons,

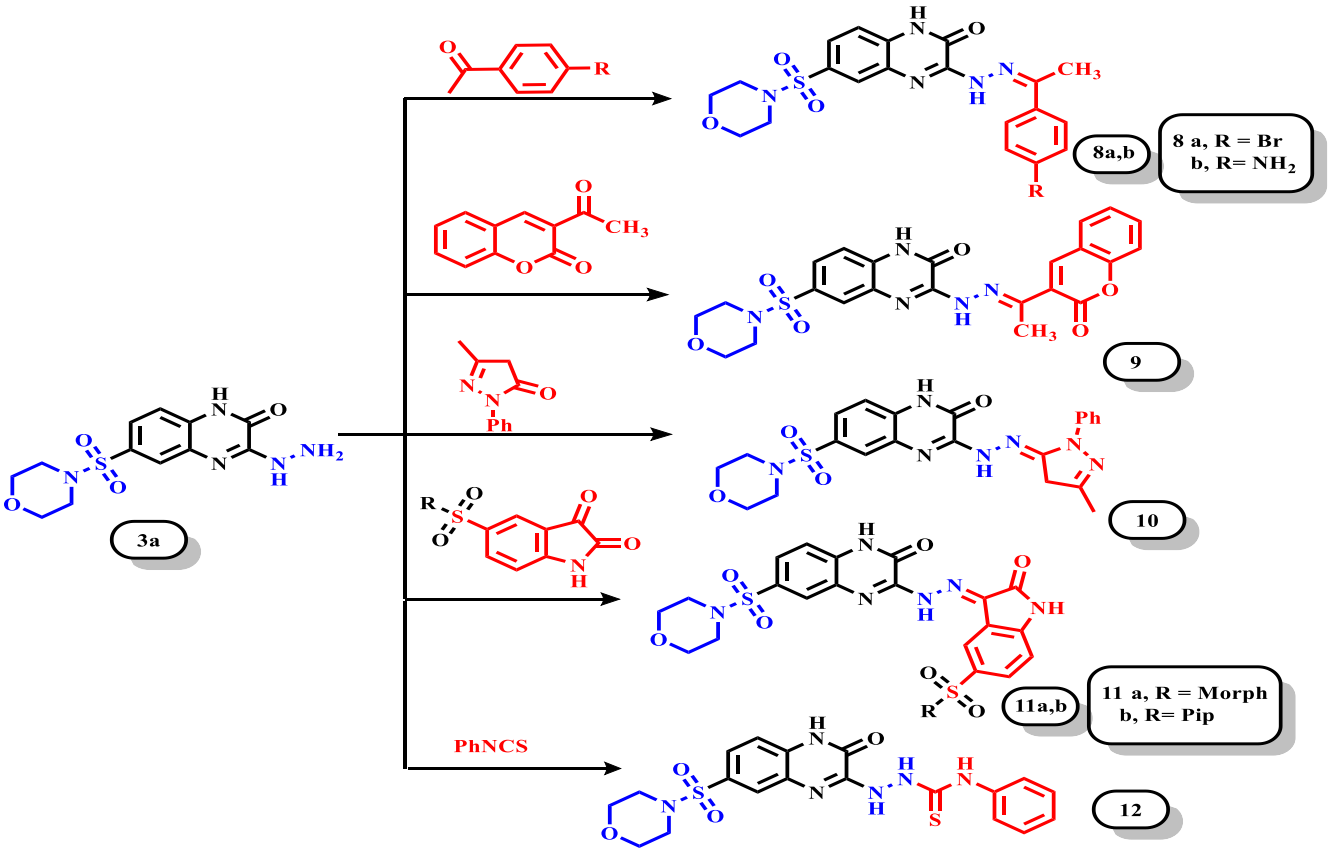

Scheme 2 Reaction of 3-(hydrazinyl)quinoxaline derivatives **3a** with some acetyl, ketone, and phenyl isothiocyanate to afford the corresponding hydrazones **7**–**11** and thiosemicarbazide derivative **12.**

besides the signals related to aromatic protons appeared at δ 7.26–8.32 ppm. The mass spectrum of compound **12** exhibited a molecular ion peak at m/z = 460 (20%) with a base peak at m/z = 74, which confirmed the molecular formula.

Furthermore, the corresponding quinoxaline derivative containing butanoic acid **13** was obtained upon the reaction of succinic anhydride with 3-(hydrazinyl)quinoxaline derivative **3a** in ethanol as solvent. The elemental analysis and spectroscopic data confirmed the prepared compound. The IR spectra of 4-oxo-butoric acid derivative **13** demonstrated absorption bands at υ 3350, 3207, and 1684 cm^{-1}, assignable to the NH and carbonyl groups. Additionally, the ^{1}H NMR spectra are characterized by the existence of four triplets at δ 2.34, 2.44, 2.86, and 3.67 ppm due to the four CH_2 groups corresponding to butanoic acid and morpholinyl moieties. Also, the CH_2 carbons of butanoic acid derivatives were observed at δ 28.42, 29.24 ppm, as well as the morpholinyl signals displayed at δ 46.29 and 65.73 ppm. Further, the two C = N and two C = O were detected at δ 155.32, 155.69, 170.38, and 174.06 ppm. The mass spectrum of 4-oxo-butric acid derivative **13** exhibited a molecular ion peak at m/z = 425 (58%) and a base peak at m/z = 259 assignable to the molecular formula $C_{16}H_{19}N_5O_7S$.

On the other hand, the starting material 3-(hydrazinyl) quinoxaline derivative **3a** reacted with either ethyl 2-cyano-3, 3-bis(methylthio)acrylate or 2-aminoprop-1-ene-1,1,3-tricarbo nitrile to afford the 1-(1,2-dihydroquinoxalin-3-yl)-1*H*-pyrazole derivative **14**, and **16**. The spectral data of pyrazole derivatives **14**, **16** are confirmed with the suggested structures. The 1-*H*-pyrazole-4-carbonitrile derivative **16** afforded stretching vibration bands of NH_2, NH, and carbonyl groups at υ 3307 and 3203 and 1684 cm^{-1}, in addition to ^{1}H NMR data exhibited a new singlet signal at δ 3.17 ppm corresponding for CH_2 of acetonitrile derivative. Also, new significant signals due to amino group at δ 7.50 ppm exchangeable with deuterated. The mass spectrum exhibited a molecular ion peak at m/z = 440 (7.0 %), characteristic of the molecular formula $C_{18}H_{16}N_8O_4S$.

Finally, the interaction of the 3-(hydrazinyl)quinoxaline derivative **3a** with dicarbonyl compounds as (ethyl acetoacetate or acetylacetone) failed to obtain the pyrazole nucleus due to the cyclization was incomplete and the corresponding hydrazone derivatives **17a, b** were obtained, as showed Scheme 3. For compound **17 a**, ^{1}H NMR spectra revealed the presence of ethoxy ester protons as triplet and quartet at δ 1.21 and 4.13 ppm, respectively. In addition, the morpholinyl protons displayed at δ 3.64, 2.89 ppm, as well as the methylene group of butanoate moiety at δ 3.58 ppm and a methyl group at δ 2.18 ppm. Further, the ^{13}C NMR spectra exhibited signals at δ 14.54, 60.94, 65,72, 46.29, 50.05, and 30.55 ppm related to ethoxy, morpholinyl, methylene, and a methyl group, respectively. Besides, signals at δ 155.71, 155.33, and 153.58 ppm corresponding to two carbonyl groups and C = N, as well as the aromatic carbons that ranged between δ 114.94–130.74 ppm.

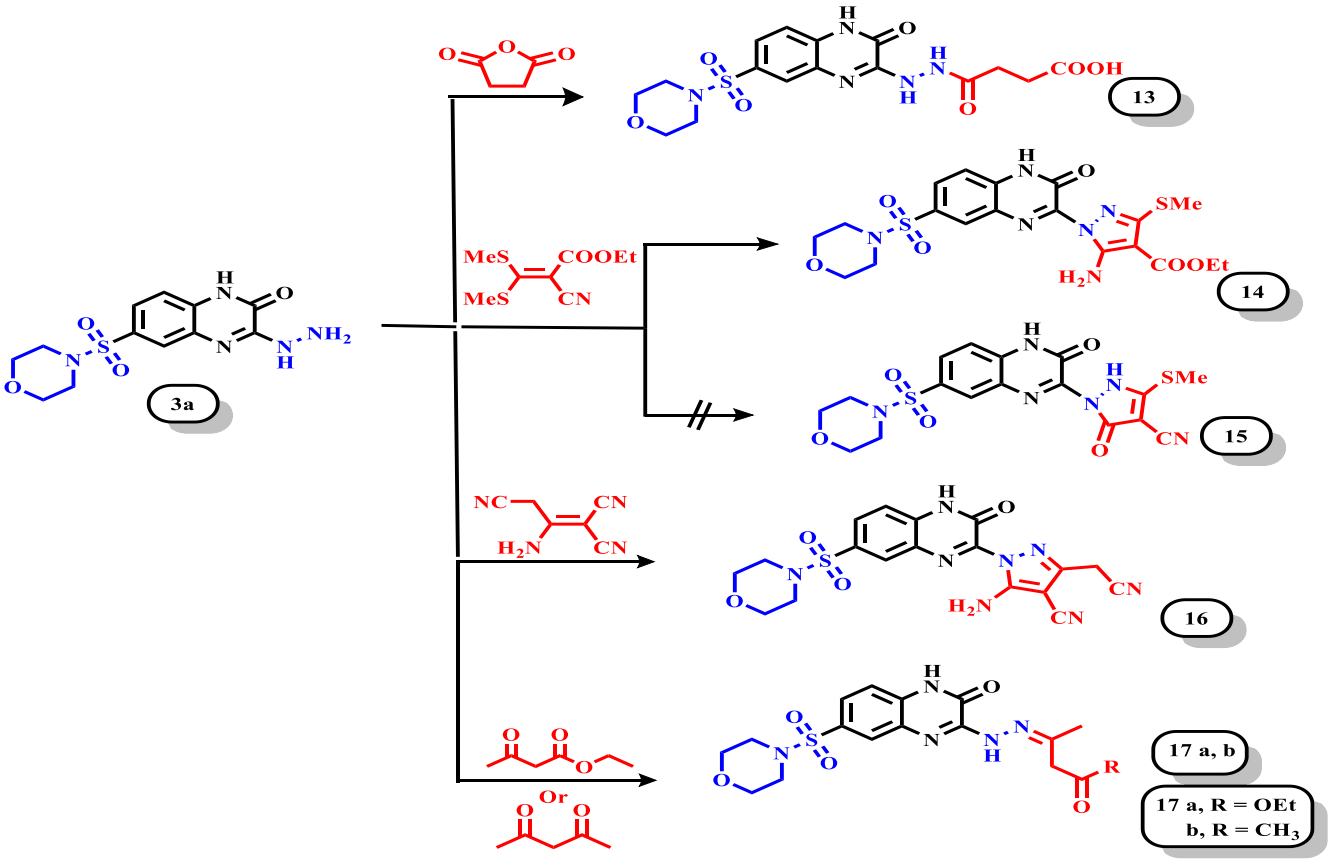

Scheme 3 Synthesis of new quinoxaline derivatives containing pyrazole **14**–**16** or hydrazone **13**, and **17a, b** moiety.

3.2. Biological activity evaluation

3.2.1. Antimicrobial activity

The newly synthesized nineteen quinoxaline derivatives containing hydrazone **4**–**11** and **17**, hydrazinyl **12**–**13**, and pyrazole **14**–**16** moieties were tested *in vitro* antimicrobial activity to evaluate and explore the relationship between antimicrobial activity and the structure. Six bacterial strains were used in this study and classified as three gram-negative strains (*E. coli* ATCC 25922, *P. aeruginosa* ATCC 27853, and *S. typhi* ATCC 6539), three gram-positive strains (*B. subtilis* ATCC 6633, *S. aureus* ATCC 29213, and *E. faecalis* ATCC 29212). Additionally, two fungal strains (*C. albicans* ATCC 10231, and *F. oxysporum* RCMB 008002) were evaluated to determine the antifungal activity. Both Tetracycline and Amphotericin B as abroad spectrum antibiotics were used as a positive control against bacterial and fungal pathogens. The antimicrobial activity was determined by measuring the inhibition zone diameters (mm) by agar well diffusion method according to the clinical and laboratory standard institute guidelines CLSI and previous methods (Ammar et al., 2016; Ammar et al., 2017). As represented in Table 1, the synthesized quinoxaline derivatives displayed good to moderate activity.

Firstly, the synthesized derivatives have higher antibacterial potential against gram-positive bacteria rather than gram-negative bacteria with the zone of inhibition (IZ) ranged between (12 ± 0.74 to 33 ± 0.53), (12 ± 0.61 to 30 ± 0.29) mm, respectively compared with Tetracycline (20 ± 0.50 to 25 ± 0.22) mm. Six quinoxaline derivatives **4a**, **7**, **8a**, **11b**, **13**, and **16** displayed better and broad antimicrobial activity against the tested strains. Among them, four quinoxaline derivatives **7**, **8a**, **11b**, and **13** showed inhibition zones ranged between (23 ± 0.65 to 32 ± 0.22) mm for gram-positive bacteria and (20 ± 0.16 to 30 ± 0.29) mm for gram-negative bacteria compared with Tetracycline (22 ± 0.25 to 25 ± 0.22) mm, and (20 ± 0.50 to 23 ± 0.20) mm for gram-positive and negative bacteria, respectively. Quinoxaline derivatives **4a**, **7**, **8a**, **11b**, and **13** exhibited the most active derivatives against *B. subtilis* with inhibition zones (IZ) (27 ± 0.50 to 32 ± 0.22), equipotent or nearly with 2-(pyrazolyl) quinoxalin-3-one derivatives **14**, **16** with IZs (25 ± 0.21, and 25 ± 0.87) in comparison to Tetracycline (25 ± 0.22). Further, 3-(hydrazono)quinoxaline-3-one derivatives **7** and **11b** showed promising activity against *S. aureus* with IZs ranged between (33 ± 0.53 to 26 ± 0.14) mm compared with Tetracycline (25 ± 0.11) mm, while quinoxaline derivatives **6** and **8b** displayed nonactivity. Besides, eight quinoxaline derivatives **4a**, **5**, **7**, **8a**, **11a**, **11b**, **13**, and **16** revealed higher inhibition zones than Tetracycline against *E. faecalis*.

Furthermore, hybridization between isatin sulfonamide and quinoxaline derivatives **11a,b** demonstrated the most active derivatives against *E. coli* with inhibition zones (27 ± 0.30, and (30 ± 0.29) mm followed by **8a** and **13** (25 ± 0.81, and 26 ± 0.11) mm and compared with Tetracycline (23 ± 0.20) mm. Also, 3-(methylene-pyrazole)hydrazinyl-quinoxaline derivative **7**, 3-(chromene-3-yl)ethylidene)hydrazinyl-quinoxa line derivative **9**, and 2(pyrazolyl)quinoxaline derivative **16** displayed inhibition zones equipotent to Tetracycline. Moreover,

Table 1 *In vitro* antimicrobial activity of the synthesized quinoxaline derivatives against different standard microbial strains.

Code	Inhibition zone represented by (mm)							
	Gram-positive			**Gram-negative**				
	B. subtilis	***S. aureus***	***E. faecalis***	***E. Coli***	***P. aeruginosa***	***S. typhi***	***C. albicans***	***F. oxysporum***
3a	20 ± 0.11	23 ± 0.29	21 ± 0. 54	22 ± 0.43	Na	15 ± 0. 36	17 ± 0.21	Na
4a	28 ± 0.16	23 ± 0. 55	25 ± 0. 3	21 ± 0.14	20 ± 0. 78	22 ± 0.12	21 ± 0. 2	17 ± 0. 45
4b	13 ± 0.25	20 ± 0.98	18 ± 0.65	16 ± 0.74	11 ± 0.54	15 ± 0.65	13 ± 0.54	15 ± 0.65
4c	14 ± 0.65	11 ± 025	15 ± 032	16 ± 0.24	14 ± 0.35	12 ± 0.68	14 ± 0.28	16 ± 0.35
5	22 ± 0.41	17 ± 0.78	25 ± 0. 14	18 ± 0.3	Na	14 ± 0. 52	19 ± 0.65	Na
6	13 ± 0.41	Na	14 ± 0. 47	19 ± 0. 33	12 ± 0. 63	Na	13.0 ± 0.2	Na
7	27 ± 0.5	26 ± 0. 14	25 ± 0. 33	23 ± 0. 14	25 ± 0. 85	23 ± 0. 11	24 ± 0. 3	20 ± 0. 82
8a	28 ± 0.5	24 ± 0. 12	29 ± 0. 55	25 ± 0.81	24 ± 0. 2	20 ± 0. 16	22 ± 0.56	18 ± 0.15
8b	15 ± 0.45	Na	12 ± 0. 74	14 ± 0.21	Na	15 ± 0. 2	12 ± 0. 65	Na
9	22 ± 0.18	22 ± 0. 34	21 ± 0. 72	23 ± 0. 44	Na	23 ± 0. 33	21 ± 0. 5	19 ± 0. 28
10	14 ± 0.24	17 ± 0.27	13 ± 0.47	20 ± 0.34	15 ± 0.46	19 ± 0.41	14 ± 0.53	17 ± 0.25
11a	23 ± 0.22	24 ± 0. 33	25 ± 0. 35	27 ± 0. 3	23 ± 0. 74	17 ± 0. 12	20 ± 0. 5	15 ± 0. 14
11b	32 ± 0.22	33 ± 0. 53	29 ± 0. 17	30 ± 0.29	27 ± 0. 73	29 ± 0.2	27 ± 0. 5	22 ± 0. 11
12	19 ± 0.65	20 ± 0.54	13 ± 0.25	17 ± 0.35	14 ± 0.45	19 ± 0.28	12 ± 0.24	16 ± 0.65
13	27 ± 0.50	25 ± 0. 77	23 ± 0.65	26 ± 0. 11	21 ± 0. 2	23 ± 0.65	25 ± 0.33	21 ± 0. 16
14	25 ± 0.21	21 ± 0. 17	19 ± 0. 14	22 ± 0. 18	17 ± 0.2	20 ± 0. 33	22 ± 0. 19	19 ± 0. 55
16	25 ± 0.87	21 ± 0.3	24 ± 0. 35	23 ± 0.2	21 ± 0.55	23 ± 0. 4	19 ± 0. 25	17 ± 0. 5
17a	18 ± 0.12	16 ± 0. 54	Na	15 ± 0. 96	Na	12 ± 0. 61	18 ± 0.2	14 ± 0. 38
17b	22 ± 0.4	20 ± 0.31	20 ± 0. 11	19 ± 0. 2	20 ± 0. 15	18 ± 0. 16	17 ± 0.35	21 ± 0.3
S1	25 ± 0.22	25 ± 0.11	22 ± 0.25	23 ± 0. 2	20 ± 0. 5	21 ± 0.55	Na	Na
S2	Na	Na	Na	Na	Na	Na	22 ± 0.2	18 ± 0.32

*Na: No activity, *S1 = Tetracycline, S2 = Amphotericin B

quinoxaline derivatives **7, 8a, 11a**, **11b**, **13**, and **16** exhibited the remarkable antibacterial activity toward *P. aeruginosa* with inhibition zones ranged between (21 ± 0.55 to 27 ± 0.73) mm in comparison to Tetracycline (20 ± 0.50) mm, while, quinoxaline derivatives **5**, **8b**, **9**, and **17a** exhibited no activity. On the other hand, quinoxaline derivatives **7**, **11b**, **13**, and **16** revealed comparable activity against *S. typhi* with a zone of inhibition ranging between (23 ± 0.11 to 29 ± 0.20) mm compared with Tetracycline with only one derivative **6** that displayed no activity.

As for antifungal activity, all the synthesized derivatives displayed activity against *C. albicans* (ATCC 10231), while **3a**, **5**, **6**, and **8b** exhibited no activity against *F. oxysporum* (RCMB 008002). Besides, the other derivatives displayed a considerable antifungal activity. Furthermore, the quinoxaline derivatives **7**, **8a**, **9**, **11a**, **11b**, and **13** revealed the highest antifungal activity against *C. albicans* (ATCC 10231) and *F. oxysporum* (RCMB 008002) pathogens with inhibition zones from (18 ± 0.15) to (27 ± 0.50) mm compared with Amphotericin B (18 ± 0.32 to 22 ± 0.20) mm.

3.2.2. Minimal inhibitory concentration (MIC) and minimal bactericidal/fungicidal concentration (MBC/MFC)

The most active quinoxaline derivatives **4a**, **7**, **8a**, **11b**, **13**, and **16** depending on the antimicrobial screening were selected to evaluate the minimal inhibitory concentrations (MIC) (μg/mL) and minimal bactericidal/fungicidal concentration (MBC/MFC) (μg/mL) as represented in Table 2. Both the MIC and MBC/MFC were determined by the conventional paper disk diffusion method and confirmed using broth microdilution procedure as described in the Clinical and Laboratory Standards Institute (CLSI) guidelines and previously reported methods (Ammar et al., 2020a, 2020b; Dias et al., 2018; Wikler, et al., 2008).

The most active derivatives **4a**, **7**, **8a**, **11b**, **13**, and **16** exhibited significant antibacterial activity with MIC values ranged between (1.95–31.25 μg/mL), (0.97–62.5 μg/mL) against gram-positive and gram-negative bacteria, respectively, and compared with Tetracycline as positive control (15.62–62.5 μg/mL). Surprisingly, 3-(2-(2-oxo-5-(piperidin-1-ylsulfonyl)indolin-3-ylidene) hydrazinyl)quinoxalin-2(1*H*)-one derivative **11b** revealed highest antibacterial potential on *B. subtilis* (MIC of 1.95 μg/mL), and *E. faecalis* (MIC of 3.9 μg/mL) in comparison to Tetracycline (MIC of 31.25 & 62.5 μg/mL). Additionally, the quinoxaline derivatives **11b** displayed the second promising derivatives against *S. aureus* with MIC value (5.57 μg/mL), after 3-(2-(1-(4-bromophenyl)ethylidene)hydrazineyl)quinoxalin-2(1*H*)-one derivative **8a** (MIC = 1.95 μg/mL) compared with Tetracycline (MIC = 62.50 μg/mL). Interestingly, quinoxaline derivatives **4a**, **7**, **8a**, **13**, and **16** exhibited considerable antibacterial activity on *B. subtilis* (MIC = 4.5, 3.9, 5.57, 9.25, 7.81 μg/mL) than Tetracycline (MIC = 31.25 μg/mL). Moreover, the quinoxaline derivatives **4a, 7, 8a, 16** showed antibacterial potential *S. aureus* (MIC of 7.81, 7.81, 1.95 & 15.62 μg/mL) compared to Tetracycline (MIC = 62.5 μg/mL). Moreover, the hydrazono-quinoxaline derivatives **4a**, **8a**, and **11b** revealed equipotent antibacterial activity on *E. faecalis* with inhibitory activity (MIC = 3.9 μg/mL) compared to Tetracycline (MIC = 62.5 μg/mL) (Fig. 2).

Furthermore, 3-(2-(2-oxo-5-(piperidin-1-ylsulfonyl)indolin-3-ylidene)hydrazinyl)-quinoxalin-2(1*H*)-one derivative **11b** showed the better antibacterial activity against *E. coli*, and *P. aeruginosa* with MIC values (0.97 and 5.57 μg/mL), respectively, in comparison to Tetracycline (MIC of 15.62 & 62.5 μg/mL). On

Table 2 Minimal inhibitory concentrations (MIC) (μg/mL) and minimum bactericidal/ fungicidal concentrations (MBC/MFC) (μg/mL) of the most active quinoxaline derivatives **4a**, **7**, **8a**, **11b**, **13**, and **16** against eight pathogenic microbes.

Cpd. No.	Test Name	Gram-positive			Gram-negative			*Fungi*	
		B. subtilis	***S. aureus***	***E. faecalis***	***E. Coli***	***P. aeruginosa***	***Salmonella typhi***	***C. albicans***	***F. oxysporum***
4a	**MIC**	**4.5**	**7.81**	**3.9**	**7.81**	**15.62**	**5.57**	**7.81**	**15.62**
	MBC	**9.2**	**15.62**	**7.41**	**14.05**	**31.25**	**10.58**	**12.49**	**26.55**
7	**MIC**	**3.9**	**7.81**	**15.62**	**7.81**	**27.77**	**18.51**	**9.25**	**31.25**
	MBC	**6.63**	**15.62**	**31.25**	**15.62**	**55.54**	**36.5**	**17.57**	**56.25**
8a	**MIC**	**5.57**	**1.95**	**3.9**	**7.81**	**31.25**	**3.9**	**15.62**	**31.25**
	MBC	**10.58**	**3.7**	**6.63**	**12.49**	**59.37**	**6.63**	**28.11**	**46.87**
11b	**MIC**	**1.95**	**5.57**	**3.9**	**0.97**	**5.57**	**7.81**	**7.81**	**15.62**
	MBC	**3.9**	**5.57**	**6.63**	**1.94**	**10.58**	**12.49**	**15.62**	**27.77**
13	**MIC**	**9.25**	**31.25**	**7.81**	**18.51**	**55.5**	**31.25**	**31.25**	**55.54**
	MBC	**18.5**	**53.12**	**15.62**	**36.5**	**88.8**	**56.25**	**41.65**	**87.5**
16	**MIC**	**7.81**	**15.62**	**9.25**	**62.5**	**31.25**	**15.62**	**31.25**	**55.54**
	MBC	**14.05**	**31.25**	**18.5**	**87.5**	**53.12**	**28.11**	**53.12**	**88.8**
Tetr.	**MIC**	**31.25**	**62.5**	**62.5**	**15.62**	**62.5**	**31.25**	**–**	**–**
	MBC	**40.62**	**87.5**	**93.75**	**18.74**	**87.5**	**43.75**	**–**	**–**
Amph. B.	**MIC**	**–**	**–**	**–**	**–**	**–**	**–**	**15.62**	**31.25**
	MFC	**–**	**–**	**–**	**–**	**–**	**–**	**34.62**	**65.62**

***Tetr**. = Tetracycline**, Amph.B** = Amphotericin B.

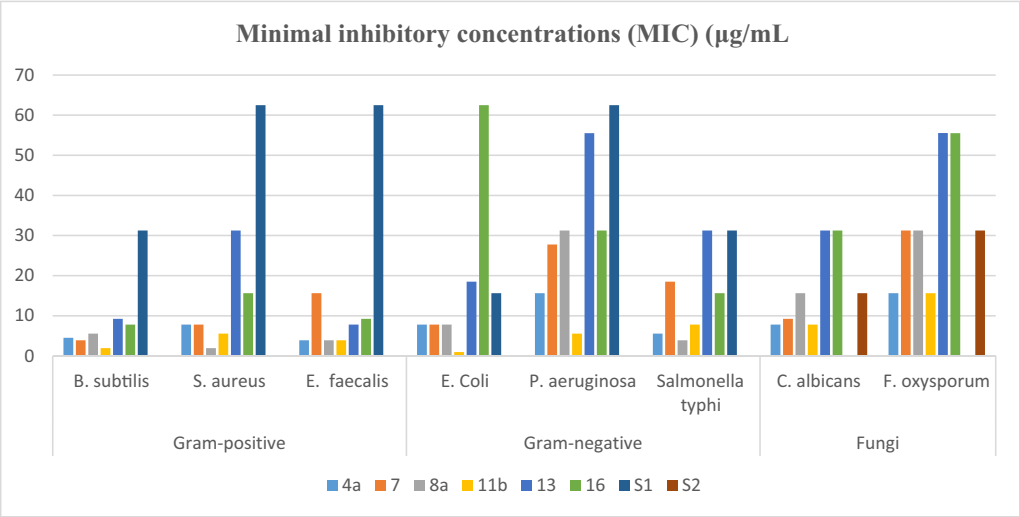

Fig. 2 Minimum inhibitory concentrations (MIC) (μg/mL) of most active 3-hydrazono-quinoxaline derivatives against pathogenic microbes.

the other hand, 3-(2-(1-(4-bromophenyl)ethylidene)hydrazineyl)-quinoxalin-2(1*H*)-one derivative **8a** demonstrated the best member antibacterial potential on *S. typhi* with inhibitory concentration (MIC = 3.9 μg/mL) in comparison to Tetracycline (MIC = 31.25 μg/mL). Additionally, 3- hydrazinylquinoxalin-2(1*H*)-one derivatives **4a**, **7**, and **8a** that are containing 4-chlorobenzylidene, (1,3-diphenyl-1*H*-pyrazol-4-yl)methylene, and 1-(4-bromophenyl)ethylidene, respectively, as variable bioactive cores showed the same antibacterial activity against *E. coli* with MIC values equal 7.81 μg/mL. Besides, these quinoxaline derivatives **4a**, **7**, and **11b** showed the best inhibitory ability against *P. aeruginosa* with MIC values (15.62, 27.77 & 5.57 μg/mL) in comparison to Tetracycline (MIC = 62.5 μg/mL). It's interesting, the presence of 4-bromophenyl derivative in 3-(2-(1-(4-bromophenyl)ethylidene)hydrazineyl)quinoxalin-2(1*H*)-one derivative **8a** exhibited the highest antibacterial activity against *S. typhi* with MIC value (3.9 μg/mL) followed by quinoxaline derivative **4a**, and **11b** (MIC = 5.57, and 7.81 μg/mL), respectively in comparison to Tetracycline (MIC of 31.25 μg/mL) (Fig. 2).

Whilst quinoxaline derivatives **4a**, and **11b** revealed strong antifungal potential with MIC values (7.81 μg/mL) against *C. albicans and* (15.62 μg/mL) against *F. oxysporum* in comparison to Amphotericin B (MIC of 15.62, 31.25, μg/mL). Further, 3-(2-(1-(4-bromophenyl)ethylidene)- hydrazineyl) quinoxalin-2(1*H*)-one derivative **8a** demonstrated equipotent to Amphotericin B against to fungal strains *C. albicans* and *F. oxysporum* with MIC values (15.62, 31.25 μg/mL),

respectively. Additionally, quinoxaline containing 4-oxo-butanoic acid derivative **13**, and 5-aminopyrazole derivative **16** exhibited lower antifungal activity with MIC values (31.25 and 55.54 μg/mL), respectively. For the *F. oxysporum* pathogen, the most active two quinoxaline derivatives **4a** and **11b** that exhibited MIC values (15.62 μg/mL), while the other hydrazono-quinoxaline derivatives **7** and **8a** showed equipotent activity in comparison to Amphotericin B with MIC value (31.25 μg/mL) (Table 2 and Fig. 2).

For further exploration, the minimal bactericidal concentration (MBC) of the most promising quinoxaline derivatives **4a, 7, 8a, 11b, 13**, and **16** were determined using the conventional paper disc diffusion method as described previously (Salem et al., 2020a, 2020b). As listed in Table 3, these derivatives revealed bactericidal/fungicidal activity with MBC values (3.7–53.12 μg/mL), (1.94–88.8 μg/mL), and MFC values (12. 49–88.8 μg/mL) against gram-positive (*B. subtilis*, *S. aureus*, and *E. faecalis*), gram-negative (*E. coli*, *P. aeruginosa*, and *S. typhi*), and fungal strains (*C. albicans* and *F. oxysporum*) compared with Tetracycline (18.74–87.5 μg/mL), and Amphotericin B (34.62–65.62 μg/mL).

The 3-(2-(2-oxo-5-(piperidin-1-ylsulfonyl)indolin-3-ylidene) hydrazinyl)-quinoxalin-2(1*H*)-one derivative **11b** displayed bactericidal concentration (MBC = 3.9, 5.57, and 6.63 μg/mL) against gram-positive strains. Besides, the hydrazono-quinoxaline derivative **11b** showed MBC values (1.94, 10.58, and 12.49 μg/mL) when tested against gram-negative strains compared with Tetracycline (MBC = 18.74–93.75 μg/mL). Interestingly, the 3-(2-(1-(4-bromophenyl)ethylidene)-hydrazi neyl)quinoxaline-2(1*H*)-one derivative **8a** displayed better bactericidal activity on *S. aureus* (MBC = 3.7 μg/mL), *E. faecalis* (MBC = 6.63 μg/mL) and *S. typhi* (MBC = 6.63 μg/mL) compared to Tetracycline (MBC of 87.5, 93.75 & 43.75 μg/mL) (Fig. 3).

The hydrazono-quinoxaline derivatives **4a**, **7**, **8a**, and **11b** revealed fungicidal activity with MFC values (12.49–56.25 μg/mL) lower than Amphotericin B (34.62–65.62 μg/mL). Furthermore, the hydrazine-quinoxaline **13**, and 3-pyrazolyl-quinoxaline **16** showed higher MFC values (41.65, 54.12 μg/mL), (87.5, and 88.8 μg/mL) against *C. albicans* and *F. oxysporum*, respectively. Among the tested derivatives, 3-(2-(4-chlorobenzylidene)hydrazineyl)quinoxalin-2(1*H*)-one derivative **4a** exhibited better fungicidal activity on *C. albicans* and *F. oxysporum* (MFC = 12.49, 26.55 μg/mL) compared to Amphotericin B (MFC = 34.62 & 65.62 μg/mL) (Fig. 3). According to the CLSI standards, it can be determined that the tested quinoxaline derivatives exhibited bactericidal/fungicidal or bacteriostatic/fungistatic depending on the values of (MBC or MFC /MIC) ratio, where if the (MBC or MFC)/MIC ratio ranged between 1 and 2 is considered as indicative cidal potential. On the other hand, for (MBC or MFC)/MIC ratio $\geq$ 8 is considered indicative of static behavior (Daschner, 1977; Guo et al., 2016; Kusakabe et al., 2019; Sun et al., 2019).

Finally, the MIC and MBC/ MFC values indicated that all the hydrazono-quinoxaline **4a**, **7**, **8a**, **11b**, hydrazine-quinoxaline **13**, and 3-pyrazolyl-quinoxalin-2-one derivative **16** exhibited bactericidal and fungicidal behavior with MBC/MIC and MFC/MIC ratio ranged between 1 and 2.

3.2.3. Drug resistance study

The most active quinoxaline derivatives **4a**, **7**, **8a**, **11b**, **13**, and **16** were further evaluated toward multidrug-resistant bacterial strains classified as gram-negative (*P. aeruginosa* ATCC BAA-2111, and *E. coli ATCC BAA*-196), and gram-positive (*S. aureus* ATCC 43300, and *S. aureus* ATCC 33591) according to previously reported methods (Ammar et al., 2021; Ragab et al., 2021). In addition, Tetracycline and Norfloxacin as broad-spectrum antibiotics were used as a positive control.

As listed in Table 3**,** the most active quinoxaline derivatives **4a**, **7**, **8a**, **11b**, **13**, and **16** revealed potent activity against all the multi-drug resistance bacteria (MDRB) strains with MIC values ranged between (1.95–15.62 μg/mL), and MBC values (3. 31–31.25 μg/mL). The 3-(2-(2-oxo-5-(piperidin-1-ylsulfonyl)in dolin-3-ylidene)hydrazinyl)-quinoxalin-2(1*H*)-one derivative **11b** exhibited the most active derivatives against three strains (*S. aureus* ATCC 43300, *P. aeruginosa* ATCC BAA-2111, and *E. coli ATCC BAA*-196) with MIC values (1.95, 1.95,

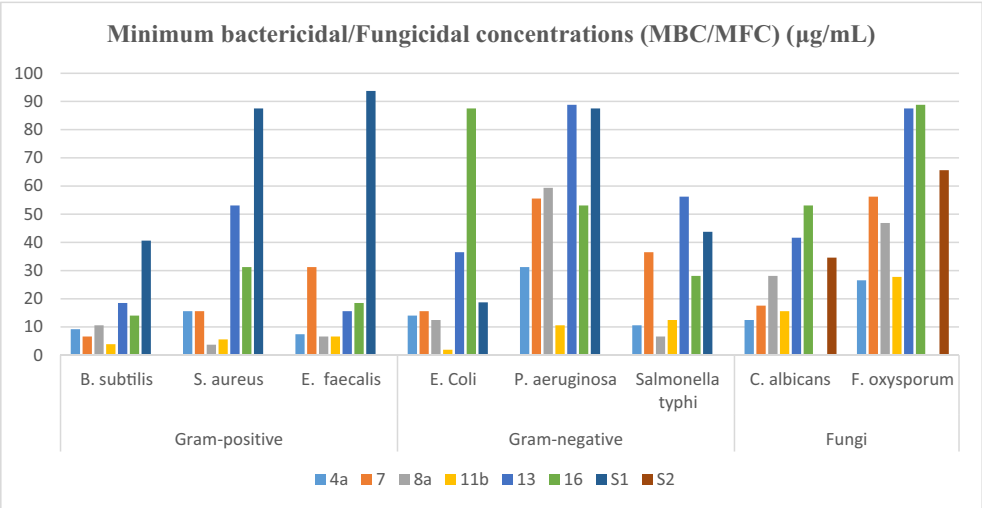

Fig. 3 Minimum bactericidal/fungicidal concentrations MBC/MFC (μg/mL) of highest activity of synthesized compounds against pathogenic microbes.

Table 3 The antimicrobial activity of the most active quinoxaline derivatives **4a**, **7**, **8a**, **11b**, **13**, and **16** against multi-drug resistant bacteria (MDRB).

Code	Mean diameter of inhibition zone (mm) and minimal inhibitory concentrations (MIC/MBC) (μg/mL)											
	***S. aureus* ATCC 43,300**			***S. aureus* ATCC 33,591**			***E. coli ATCC BAA*-196**			***P. aeruginosa* ATCC BAA-2111**		
	IZ	MIC	MBC	IZ	MIC	MBC	IZ	MIC	MBC	IZ	MIC	MBC
4a	26 ± 0.71	6.25	11.87	15 ± 0.4	8.88	15.98	20 ± 0.33	9.25	18.5	21 ± 0.3	7.81	15.62
7	24 ± 0. 5	4.44	8.88	25 ± 0.2	1.95	3.31	23 ± 0. 14	6.25	11.87	24 ± 0.18	5.2	8.61
8a	25 ± 0.45	3.9	7.41	23 ± 0.4	5.55	11.1	22 ± 0.2	7.81	15.62	24 ± 0.16	4.44	6.66
11b	27 ± 0.33	1.95	3.9	24 ± 0.2	3.9	7.8	25 ± 0.16	1.95	3.9	26 ± 0. 44	3.9	7.8
13	17 ± 0.45	15.62	31.25	22 ± 0.45	3.9	7.41	19 ± 0.81	9.25	18.5	23 ± 0. 5	15.62	31.25
16	20 ± 0. 3	7.81	15.62	21 ± 0. 15	9.25	18.5	22 ± 0.15	3.9	7.41	19 ± 0. 66	6.25	11.87
Tetr.	–	–		–	–		–	–		–	–	
Nor.	25 ± 0.5	1.25	2.5	26 ± 0.5	0.78	1.4	27 ± 0.98	1.57	2.66	24 ± 0.47	3.13	5.32

and 3.9 μg/mL) ,and MBC values (3.9, 3.9, and 7.8 μg/mL) in comparison to Tetracycline that observed no activity and Norfloxacin MICs (1.25, 0.78, and 3.13 μg/mL), and MBCs (2.5, 1.40, and 5.32 μg/mL). Additionally, the 3-(2-((1,3-diphenyl-1*H*-pyrazol-4-yl)methylene)hydrazineyl)quinoxalin-2(1*H*)-one derivative **7** showed the best antibacterial activity against *S. aureus* (ATCC 33591) with MIC values (1.95 μg/mL), and MBC values (3.9 μg/mL) comparison to Norfloxacin (MIC = 1.57 μg/mL, and MBC = 2.66 μg/mL).

Finally, the structure–activity relationship (SAR) indicated that 6-(morphilionsulfonyl)quinoxaline linked to hydrazine, hydrazone, and pyrazolyl moieties had a profound effect on the antibacterial action, especially multi-drug resistance bacteria strains. Furthermore, hydrazono-quinoxaline derivatives **11b** revealed the best activity toward multi-drug resistance bacteria compared to Norfloxacin, which may be due to the presence of indolinyl and piperidinyl moieties in position three. Similarly, the other quinoxaline derivatives showed a considerable antibacterial potential against multi-drug resistance strains and displayed MIC and MBC values near-standard Norfloxacin. Moreover, the MBC/MIC ratios of the most active derivatives and Norfloxacin against MDRB exhibited bactericidal behavior.

3.2.4. DNA gyrase inhibition activity

DNA gyrase is an essential bacterial enzyme that belongs to topoisomerase enzymes involved in controlling topological transitions of DNA. It can inhibit bacterial growth by two different mechanisms as inhibiting the ATPase activity of gyrase blocks the introduction of negative supercoils in DNA as amino coumarin or by direct DNA gyrase inhibition as Ciprofloxacin (gyrase poisoning) that may have an impact on cell physiology and division (Collin et al., 2011).

To explore the mode of action for the most active quinoxaline derivatives **4a**, **7**, **8a**, **11b**, **13**, and **16**, the *S. aureus* DNA gyrase inhibition activity expressed by IC_{50} (μM) were performed and represented in Table 4 and Fig. 4. The Ciprofloxacin was used as positive control. The order of DNA gyrase inhibitory potential can be represented as **11b** < **7** < **8a** < **4a** < **16** < **13**. The 3-(2-(2-oxo-5-(piperidin-1-ylsulfonyl)indolin-3-ylidene)hydrazinyl)-quinoxalin-2(1*H*)-one derivative **11b** and 3-(2-((1,3-diphenyl-1*H*-pyrazol-4-yl)methylene)hydrazineyl)quinoxalin-2(1*H*)-one derivative **7** showed better activity with inhibitory (IC_{50} = 10.93 ± 1.81 & 15.83 ± 1.55 μM), respectively compared to Ciprofloxacin (IC_{50} = 26.31 ± 1.64 μM).

Table 4 Determination of the *S. aureus* DNA gyrase inhibitory activity IC_{50} (μM) of most active quinoxaline derivatives **4a**, **7**, **8a**, **11b**, **13**, and **16**.

Compound	*S. aureus* DNA gyrase Supercoiling IC_{50} (μM)
4a	**20.05 ± 1.45**
7	**15.83 ± 1.55**
8a	**16.56 ± 1.12**
11b	**10.93 ± 1.81**
13	**26.18 ± 1.22**
16	**23.47 ± 1.23**
Cip.	**26.31 ± 1.64**

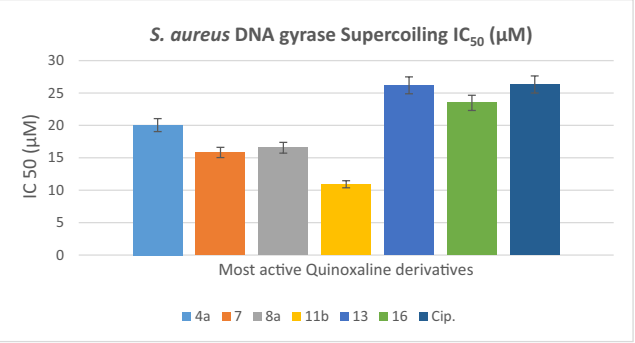

Fig. 4 Determination of the *S. aureus* DNA gyrase inhibitory activity of the most active quinoxaline derivatives.

Meanwhile, the 3-(2-(4-chlorobenzylidene)hydrazineyl)quinoxalin-2(1*H*)-one derivative **4a** displayed (IC_{50} = 20.05 ± 1.45 μM), while the 3-(2-(1-(4-bromophenyl)ethylidene)hydrazineyl)quinoxalin-2(1*H*)-one derivative **8a** showed DNA gyrase inhibitory potential (IC_{50} = 16.56 ± 1.12 μM). This difference in IC_{50} values (nearly 3.49 μM) and activity (MIC, MBC) between the two quinoxaline derivatives **4a**,

Table 5 Intracellular killing activities of active compounds.

Compound	Intracellular killing activity %
4a	**113.2 ± 0. 5**
7	**116.7 ± 0. 14**
8a	**136.5 ± 0.3**
11b	**142.4 ± 0.98**
13	**82.8 ± 0.37**
16	**98.7 ± 0. 19**

and **8a** may be related to the presence of excess methyl group and replace the choro by bromo atom in hydrazono-quinoxaline derivative **8a**. Additionally, the 3-(1*H*-pyrazole)-2-oxoquinoxaline derivative **16** showed DNA gyrase inhibitory activity (IC_{50} = 23.47 ± 1.23 μM), while 3-(hydrazino) quinoxaline derivative **13** revealed the lowest activity (IC_{50} = 26.18 ± 1.22 μM), but still more active than Ciprofloxacin (IC_{50} = 26.31 ± 1.64 μM).

3.2.5. Immunomodulatory activity for most potent compounds

Our work was extended to study the *in vitro* immunomodulatory activity of the most active quinoxaline derivatives **4a**, **7**, **8a**, **11b**, **13**, and **16** using nitro-blue tetrazolium (NBT) reduction according to the reported method (Baehner,0.1968, and Salem et al., 2020a). The immunomedioratory activity is expressed as the intracellular killing percentage (%) values represented in Table 5. The NBT assay was evaluated for most active compounds and the results represented an increase in neutrophil killing capabilities. Additionally, an increased intracellular killing percentage related to an enhancement in the killing ability toward neutrophils.

The quinoxaline derivatives **4a**, **7**, **8a**, **11b**, **13**, and **16** revealed as good immunomedioratory agents by percentage ranged between 82.8 ± 0.37 to 142.4 ± 0.98 %. Interestingly, hydrazono-quinoxaline with isatin sulfonamide **11b** showed the highest immunomedioratory derivative with intracellular killing percentages (142.4 ± 0.98) %. The order of intracellular killing percentages can be represented as **11b** < **8a** < **7** < **4a** < **16** < **13**. The quinoxaline derivatives **8a**, **7**, **4a**, **16**, and **13** displayed a good immunostimulatory potential with ratio (136.5 ± 0.3, 116.7 ± 0. 14, 113.2 ± 0. 5, 98.7 ± 0. 19, and 82.8 ± 0. 37) %, respectively.

3.2.6. In silico ADME study

Some physicochemical properties of the most active quinoxaline derivatives **4a**, **7**, **8a**, **11b**, **13**, and **16** were calculated using the Molinspiration cheminformatics web tool as represented previously (https://www.molinspiration.com/) (Salem et al., 2020a). Among the physicochemical parameters, the molecular weight (M. wt.), n-octanol–water partition coefficient (MlogP), number of hydrogen bond acceptors (nHBA), number of hydrogen bond donor (nHBD), number of rotatable bonds (*n*RB), and topological polar surface area (TPSA) were calculated to determine if the most active derivatives obey Lipinski's and Veber rule in Drug-likeness or not. According to Lipinski's rule, the drug can follow this role when observed one or no violation. Lipinski's rule involved (molecular weight < 500 Dalton, *M*LogP ≤ 4.15, *n*HBA ≤ 10, and nHBD ≤ 5). From Table 6, the results observed that the quinoxaline derivatives **4a**, **8a**, **13**, and **16** obeyed Lipinski's rule of five without violation, similarly to Norfloxacin and Ciprofloxacin as the positive control. In contrast, the hydrazono-quinoxaline derivatives **7**, and **11b** exhibited violations from Lipinski's due to the molecular weight higher than 500 Dalton and the number of hydrogen bonds more than ten.

It's interesting to know that both topological polar surface area (TPSA) and the number of rotatable bonds (*n*RB) are very useful physicochemical parameters for the prediction of drug transport properties and good descriptors of oral bioavailability of drugs (Z El-Attar et al., 2018). Additionally, for a drug that can obey the Veber rule when a number of rotatable bonds are less than ten and TPSA < 140 $Å^2$. Further, quinoxaline derivatives **4a**, **7**, and **8a** follow the Veber rule, while **11b**, **13**, and **16** have one violation from the Veber rule by displayed TPSA > 140 $Å^2$.

Furthermore, bioavailability score, synthetic accessibility, and some pharmacokinetic properties for the most active and positive control were calculated using the SwissADME web tool (http://swissadme.ch/index.php) according to the previously reported method (Fayed et al., 2020). The quinoxaline derivatives revealed bioavailability scores ranged between 0.11 and 0.55 compared with Norfloxacin and Ciprofloxacin 0.55. Besides, easy synthetic accessibility ranged between 3.48 and 4.35 compared to Norfloxacin (2.46) and Ciprofloxacin (2.51).

From Table 7, we found that all the quinoxaline derivatives are substrates of P-gp protein and, therefore, can efflux out of the cell except hydrazino-quinoxaline derivatives **13**. Surpris-

Table 6 *In silico* prediction of physicochemical, drug-likeness properties, and medicinal chemistry parameters of most active quinoxaline derivatives.

Cpd. No.	M.wt.	*M*LogP	*n*HBA	nHBD	*n*RB	TPSA	Bioavailability Score	Synthetic accessibility
4a	447.90	1.96	9	2	5	116.76	0.55	3.48
7	555.61	2.61	11	2	7	134.59	0.17	4.21
8a	506.37	2.54	9	2	5	116.76	0.55	3.60
11b	601.65	1.25	14	3	6	187	0.17	4.35
13	425.42	−1.28	12	4	7	170.79	0.11	3.58
16	440.44	−0.37	12	3	4	183.80	0.55	3.64
Nor.	319.33	−0.69	6	2	3	74.57	0.55	2.46
Cip.	331.34	−0.70	6	2	3	74.57	0.55	2.51

Table 7 *In silico* some pharmacokinetic properties and toxicity prediction of the most quinoxaline derivatives as well as standard drugs.

Cpd. No.	Pharmacokinetics			Oral toxicity prediction					
	GI Abs.	**BBB Pert.**	**P-gp Sub.**	**LD_{50} mg/kg**	**Toxicity Class**	**Carcino.**	**Immuno.**	**Mutagen.**	**Cyto.**
4a	High	No	Yes	3000	V	Inactive 0.57	Inactive 0.93	Inactive 0.74	Inactive 0.77
7	Low	No	Yes	1400	IV	Inactive 0.52	Inactive 0.90	Inactive 0.70	Inactive 0.72
8a	High	No	Yes	1600	IV	Inactive 0.57	Inactive 0.88	Inactive 0.72	Inactive 0.74
11b	Low	No	Yes	3000	V	Inactive00.52	Inactive 0.76	Inactive 0.70	Inactive 0.69
13	Low	No	No	1000	IV	Inactive 0.52	Inactive 0.99	Inactive 0.71	Inactive 0.60
16	Low	No	Yes	1800	IV	Inactive 0.51	Inactive 0.99	Inactive 0.68	Inactive 0.65
Nor.	High	No	Yes	1000	IV	Inactive 0.57	Inactive 0.98	Inactive 0.92	Inactive 0.90
Cip.	High	No	Yes	2000	IV	Inactive 0.57	Inactive 0.91	Active 0.75	Inactive 0.92

Gastrointestinal absorption = GI Abs.; blood–brain barrier permeant = BBB Permeant; P-glycoprotein substrates = P-gp Substrate; Carcino. = Carcinogenicity; Immuno. = Immunotoxicity; Mutagen = Mutagenicity; Cyto. = Cytotoxicity

ingly, the most promising quinoxaline derivatives, Norfloxacin, and Ciprofloxacin showed no permeant to the blood–brain barrier. In addition, the quinoxaline derivatives **4a**, and **8a** besides Norfloxacin and Ciprofloxacin displayed Gastrointestinal high absorption, while the quinoxaline derivatives **7**, **11b**, **13**, and **16** exhibited Gastrointestinal low absorption.

The importance of toxicity prediction in drug design is related to reducing the number of animal experiments. The most active derivatives **4a**, **7**, **8a**, **11b**, **13**, and **16** and Norfloxacin, as well as Ciprofloxacin, were exported as a smile to ProTox-II web tool (https://tox-new.charite.de/protox_II/) (Banerjee et al., 2018), to evaluate carcinogenicity, immunotoxicity, mutagenicity, cytotoxicity, and lethal dosage 50 (LD_{50}) expressed by mg/kg. The tested derivatives **4a**, **7**, **8a**, **11b**, **13**, and **16** exhibited non-carcinogenic, non-immunotoxin, and non-cytotoxic with confidence values ranging between (0.51–0.57, 0.76–0.99, and 0.60–0.77), respectively. Additionally, these derivatives exhibited inactive against mutagenicity with confidence values ranged between (0.68–0.74) compared with Norfloxacin that displayed inactive with confidence value (0.92), while Ciprofloxacin was expected to have mutagenic properties.

Our work extended to study the lethal dosage 50 (LD_{50}) meaning the dose at which 50% of test subjects die upon exposure to a drug. The LD_{50} expressed by mg/kg and according to the globally harmonized system of classification of labelling of chemicals (GHS) (Miyagawa, 2010) classified to six classes as [Class I: fatal if swallowed ($LD_{50} \leq 5$), Class II: fatal if swallowed ($5 < LD_{50} \leq 50$), Class III: toxic if swallowed ($50 < LD_{50} \leq 300$), Class IV: harmful if swallowed ($300 < LD_{50} \leq 2000$), Class V: may be harmful if swallowed ($2000 < LD_{50} \leq 5000$), Class VI: non-toxic ($LD_{50} > 5000$)]. The most active quinoxaline derivatives demonstrated predicted LD_{50} values ranged between (1000–3000 mg/kg), compared with Norfloxacin (LD_{50} = 1000 mg/kg), and Ciprofloxacin (LD_{50} = 2000 mg/kg). In addition, the tested quinoxaline derivatives and positive controls belong to class IV, except hydrazono-quinoxaline derivatives **4a** and **11b** appertain to class V (Table 8).

Finally, it can be concluded that the most active quinoxaline derivatives displayed good drug-likeness, some pharmacokinetics, and oral bioavailability properties, besides non-toxicity prediction with safety LD_{50} values.

3.2.7. Molecular docking study

Molecular docking simulations of most active quinoxaline derivatives **4a**, **7**, **8a**, **11b**, **13**, and **16** were performed inside the active site of *S. aureus* DNA gyrase (PDB: 2XCT) according to the reported method (Ragab et al., 2021). The docking study was achieved using Molecular Operating Environmental (MOE) 10.2008 (Eissa et al., 2021). The docking results showed good binding between the tested derivatives and active site in the pocket with lower binding energy ranged between S = – 17.38 to –23.81 Kcal/mol, compared with co-crystallized ligand Ciprofloxacin S =- 13.65 Kcal/mol. Additionally, the quinoxaline derivatives displayed two types of intersections as Hydrogen bond or arene-cation interaction.

The most active hydrazone derivatives **11b** depending on the IC_{50} values of DNA gyrase (IC_{50} = 10.93 ± 1.81 μM), that containing two bioactive cores (isatin sulfonamide and quinoxaline sulfonamide) exhibited the lowest binding energy S = –23.81 Kcal/mol with three hydrogen bonds and one arene-cation interaction. The hydrogen bonds formed between the resides Lys1043 with the oxygen of morpholinyl group, Lys460 with the carbonyl of quinoxaline, and Glu435 with NH of isatin derivative with bond length 3.66, 2.47, and 2.70 ˚A, respectively (Figs. 5a and b).

Furthermore, 3-(2-((1*H*-pyrazol-4-yl)methylene)hydrazineyl)quinoxalin-2(1*H*)-one derivative **7** demonstrated binding energy S = –22.12 Kcal/mol through only one hydrogen bond backbone donor between Arg1033 and NH of hydrazinyl quinoxaline derivative with bond length 2.90 ˚A, and strength 13%. Besides, two arene-cation interactions between

Table 8 Binding energy and interaction details of the most active quinoxaline derivatives **4a**, **7**, **8a**, **11b**, **13**, and **16** inside the active site of *S. aureus* DNA gyrase (PDB: 2XCT).

Cpd. No.	S (Kcal/mol)	Residues	Interacting group	Type of H-bond	Strength %	Length ˚A
4a	−20.11	Arg1048	Oxygen of morpholinyl	Acceptor	23	3.16
		Arg1048	Oxygen of morpholinyl	Acceptor	34	3.04
		Ser1028	Oxygen of sulfonyl group	acceptor	65	2.71
		Asp510	NH of hydrazine derivative	Donor	38	3.36
		Lys460	4-chlorophenyl derivative	-	-	-
7	–22.12	Arg1033	NH of hydrazine derivative	Donor	13	2.90
		Arg1033	Phenyl of quinoxaline	-	-	-
		Arg1092	Phenyl at N1 of pyrazole derivative	-	-	-
8a	−21.20	Arg1048	Oxygen of morpholinyl	Acceptor	52	2.75
		Arg1048	Oxygen of morpholinyl	Acceptor	16	3.13
		Ser1028	Oxygen of sulfonyl	Acceptor	93	2.67
11b	–23.81	Lys1043	Oxygen of morpholinyl	Acceptor	11	3.66
		Lys460	Carbonyl of quinoxaline	Acceptor	41	2.47
		Glu435	NH of isatin	Donor	60	2.70
		Arg1033	Phenyl of quinoxaline	-	-	-
13	−17.38	Arg1048	Oxygen of morpholinyl	Acceptor	60	2.55
16	−18.96	Arg1048	Cyano of acetonitrile derivative	Acceptor	27	2.89
		Arg1048	Cyano of acetonitrile derivative	Acceptor	28	3.04
		Arg1033	Cyano at position four at pyrazole ring	acceptor	44	2.78
Cip	−13.65	His1081	Oxygen of carboxylate	Acceptor	37	2.30
		Tyr580	NH of piperazine	Donor	48	2.55

Cip. = **Ciprofloxacin**; (-) = **meaning arene-cation interaction**

Arg1033, Arg1092 with phenyl of quinoxaline, and phenyl at *N1* of pyrazole derivatives, respectively.

Moreover, the 3-(2-(1-(4-bromophenyl)ethylidene)hydrazi neyl)quinoxalin-2(1*H*)-one derivative **8a** observed binding energy S = -21.20 Kcal/mol with three hydrogen bonds side-chain acceptor with bond length ranged between 2.67 and 3.13 ˚A through two residues Arg1048 and Ser1028. The residues Arg1048 formed two hydrogen bonds with the oxygen of morpholinyl with bond length and strength 2.75 ˚A (52%), and 3.13 ˚A (16%) (Figs. 6a and b). Additionally, the hydrazino-quinoxaline derivative **13** observed the less active member in our study with binding energy S = -17.38 Kcal/mol through forming one hydrogen bond between the residue Arg1048 and oxygen of morpholinyl with bond length 2.55

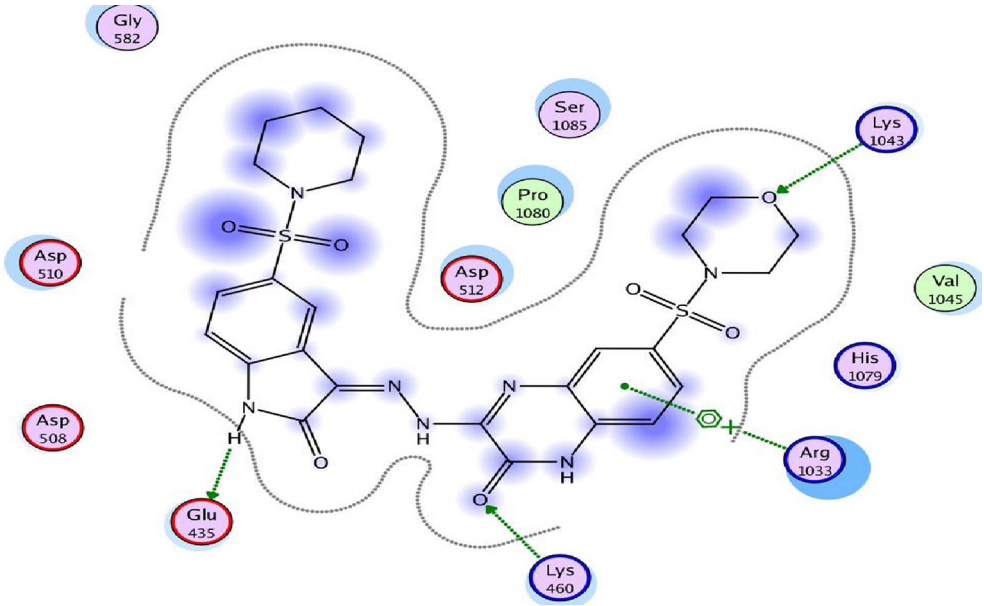

Fig. 5a 2D interaction between the quinoxaline derivative **11b** and the active site of DNA gyrase (2XCT).

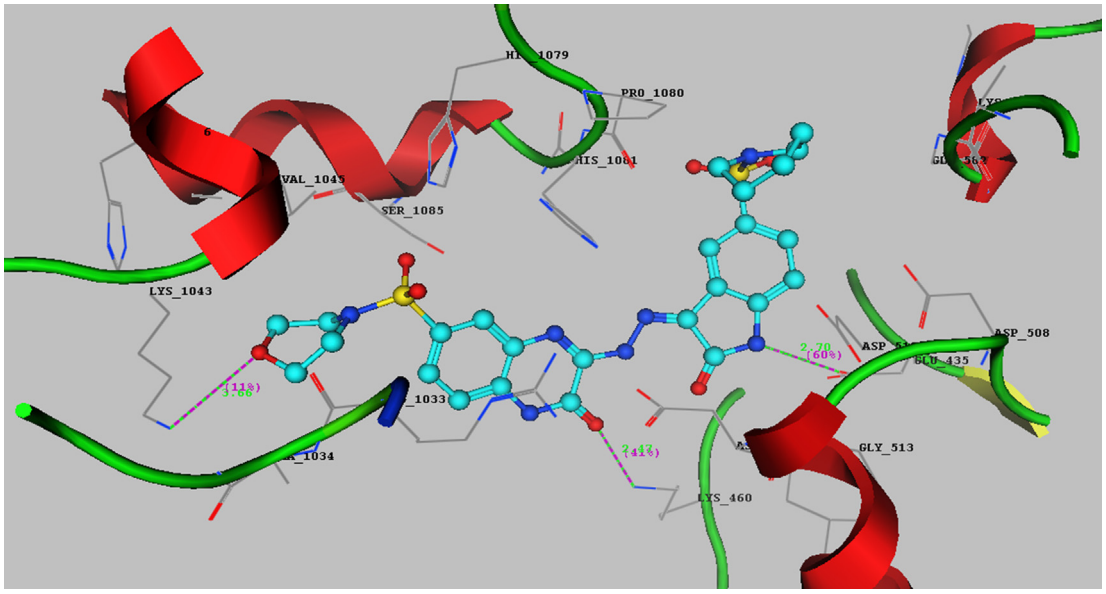

Fig. 5b 3D interaction between the quinoxaline derivative **11b** and the active site of DNA gyrase (2XCT).

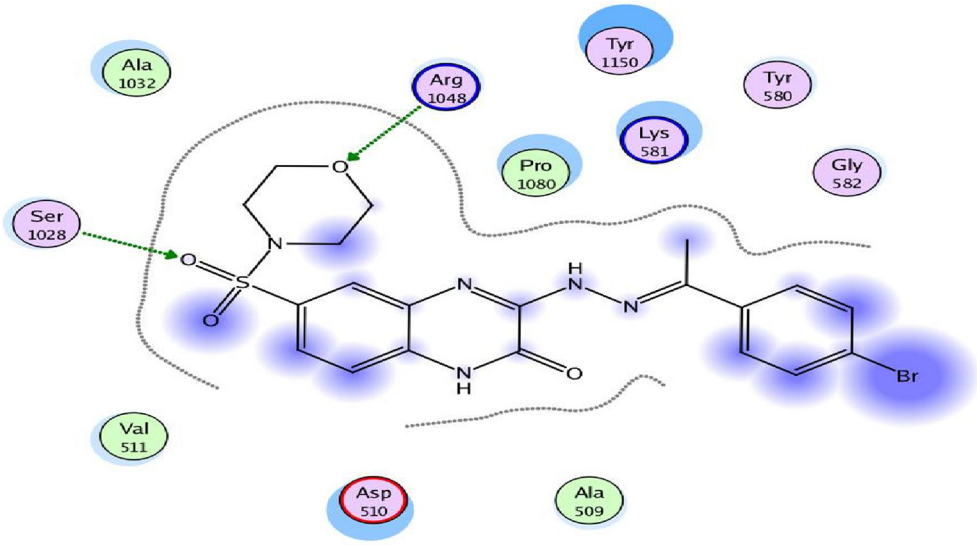

Fig. 6a 2D interaction between the quinoxaline derivative **8a** and the active site of DNA gyrase (2XCT).

Å and strength 60%. On the other hand, the 2-pyrazolyl-2-oxoquinoxaline derivative **16** showed binding energy S = -18.96 Kcal/mol with three hydrogen bonds sidechain acceptor. Similarly, the 3-(2-(4-chlorobenzylidene)hydrazineyl)quinoxalin-2(1*H*)-one derivative **4a** exhibited binding energy S = -20.11 Kcal/mol with two hydrogen bonds sidechain acceptor between Arg1048 and the oxygen of morpholinyl and one hydrogen bond acceptor between Ser1028 and oxygen of sulfonyl with bond length 3.16, 3.04, 2.71 Å, respectively. Besides, one hydrogen bond sidechain acceptor between Asp510 with NH of hydrazino-quinoxaline derivative with bond length 2.36 Å and strength 38%, as well as arene-cation interaction between Lys460 and phenyl of 4-chlorophenyl derivative. (All docking figures were represented in the supplementary material file).

4. Conclusion

The present study reported the synthesis of nineteen quinoxalin-2(1*H*)-one derivatives containing hydrazone, hydrazine, and pyrazole moieties were developed and synthesized. The newly synthesized nineteen quinoxaline derivatives containing hydrazone **4–11** and **17**, hydrazinyl **12–13**, and pyrazole **14–16** moieties were tested *in vitro* antimicrobial activity to evaluate the antimicrobial activity. The synthesized derivatives have higher antibacterial potential against

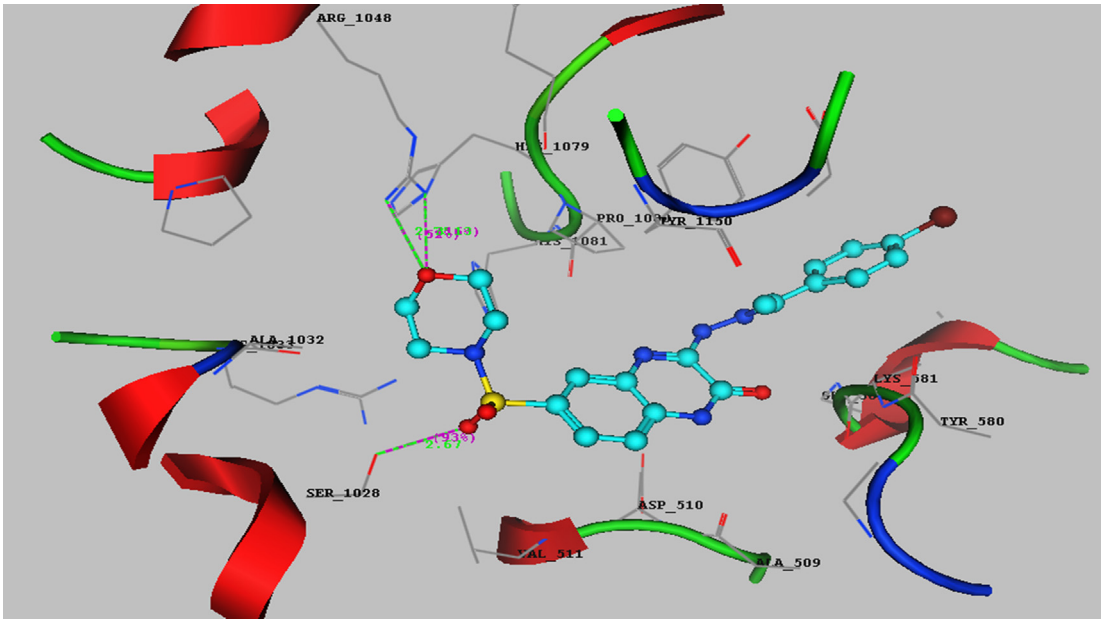

Fig. 6b 3D interaction between the quinoxaline derivative **8a** and the active site of DNA gyrase (2XCT).

gram-positive bacteria rather than gram-negative bacteria with a zone of inhibition (IZ) ranged between (12 ± 0.74 to 33 ± 0.53), (12 ± 0.61 to 30 ± 0.29) mm, respectively compared with Tetracycline (20 ± 0.50 to 25 ± 0.22) mm. Six quinoxaline derivatives **4a**, **7**, **8a**, **11b**, **13** and **16** displayed better and broad antimicrobial activity against the tested strains. The most active derivatives **4a**, **7**, **8a**, **11b**, **13** and **16** exhibited significant MIC values ranged between (1.95–31.25 μg/mL), (0.97–62.5 μg/mL) against gram-positive and gram-negative bacteria, respectively, and compared with Tetracycline as positive control (15.62–62.5 μg/mL). Additionally, these derivatives revealed bactericidal activity with MBC values (3.7–53. 12 μg/mL) against gram-positive strains (*B. subtilis*, *S. aureus*, and *E. faecalis*), and MBC values (1.94–88.8 μg/mL) against gram-negative strains (*E. coli*, *P. aeruginosa*, and *S. typhi*) compared with Tetracycline (40.62–93.75 μg/mL), and (18.7 4–87.5 μg/mL), respectively. Besides, fungicidal activity with MFC values (12.49–88.8 μg/mL) against fungal strains (*C. albicans* and *F. oxysporum*) in comparison to Amphotericin B (34.62–65.62 μg/mL). The MBC/MIC and MFC/MIC ratio ranged between 1 and 2 and exhibited bactericidal and fungicidal potency. Also, the most active quinoxaline derivatives **4a**, **7**, **8a**, **11b**, **13** and **16** revealed potent activity against all the multi-drug resistance bacteria (MDRB) strains with MIC values ranged between (1.95–15.62 μg/mL), and MBC values (3.31–31.25 μg/mL). The hydrazono-quinoxaline derivatives **11b** revealed the best activity toward multi-drug resistance bacteria with MIC values (1.95, 1.95, 3.9 μg/mL) ,and MBC values (3.9, 3.9, 7.8 μg/mL) in comparison to tetracycline that observed no activity and Norfloxacin MICs (1.25, 0.78, 3.13 μg/mL), ad MBCs (2.5, 1.40, and 5.32 μg/mL). This good activity may be a result of the presence of indolinyl and piperidinyl moieties in position three. The most active quinoxaline derivatives **4a**, **7**, **8a**, **11b**, **13** and **16** were evaluated against *S. aureus* DNA gyrase inhibition assay with IC_{50} values (10.9 3 ± 1.81–26.18 ± 1.22 μM) compared with Ciprofloxacin (26.31 ± 1.64 μM) and the order of DNA gyrase inhibitory potential can be represented as **11b** < **7** < **8a** < **4a** < **16** < **13**. Further, these quinoxaline derivatives could increase intracellular killing percentage and therefore display immunomedioratory activity. Furthermore, the most promising derivatives were performed in silico ADME and toxicity prediction. Most of them showed agreement to Lipinski's and Veber's rules with good drug-likeness, some pharmacokinetic, and oral bioavailability properties. Besides, these derivatives showed non-carcinogenic, non-immunotoxin, non-mutagenic, and non-cytotoxic prediction with safety LD values. Additionally, the molecular docking study displayed lower binding energy with good binding mode and different interaction types with bond length lower than 3.40 ˚A. Finally, this study identifies 6-(morpholinosulfonyl)quinoxalin-2(1H)-one derivatives that can contribute to developing new antibacterial agents with DNA gyrase inhibitory and immunomodulatory potential.

Acknowledgements

Taif University Researchers Supporting Project number (TURSP-2020/220), Taif University, Taif, Saudi Arabia.

Appendix A. Supplementary material

Supplementary data to this article can be found online at https://doi.org/10.1016/j.arabjc.2021.103497.

References

Ali, I.A.I., Al-Masoudi, I.A., Hassan, H.G., Al-Masoudi, N.A., 2007. Synthesis and anti-HIV activity of new homo acyclic nucleosides, 1-(pent-4-enyl) quinoxalin-2-ones and 2-(pent-4-enyloxy) quinoxalines. Chem. Heterocycl. Compd. 43, 1052–1059.

Almeida, S.T., Paulo, A.C., Babo, J., Borralho, J., Figueiredo, C., Gonçalves, B., Lança, J., Louro, M., Morais, H., Queiroz, J., de Lencastre, H., Sá-Leão, R., 2021. Absence of methicillin-resistant

Staphylococcus aureus colonization among immunocompetent healthy adults: Insights from a longitudinal study. PLoS One 16, e0253739.

Alt, S., Mitchenall, L.A., Maxwell, A., Heide, L., 2011. Inhibition of DNA gyrase and DNA topoisomerase IV of Staphylococcus aureus and Escherichia coli by aminocoumarin antibiotics. J. Antimicrob. Chemother. 66, 2061–2069. https://doi.org/10.1093/jac/dkr247.

Ammar, Y.A., AM, S., El-Sharief, M., M Ghorab, M., A Mohamed, Y., Ragab, A., Y Abbas, S., 2016. New imidazolidineiminothione, imidazolidin-2-one and imidazoquinoxaline derivatives: synthesis and evaluation of antibacterial and antifungal activities. Curr. Org. Synth. 13, 466–475.

Ammar, Y.A., Abbas, S.Y., El-Sharief, M.A.M.S., Salem, M.A.E.-R., Mohamed, A.R., 2017. Synthesis and characterization of new imidazolidineiminothione and bis-imidazolidineiminothione derivatives as potential antimicrobial agents. Eur. J. Chem. 8, 76–81. https://doi.org/10.5155/eurjchem.8.1.76-81.1542.

Ammar, Y.A., El-Hafez, S.M.A.A., Hessein, S.A., Ali, A.M., Askar, A.A., Ragab, A., 2021. One-pot strategy for thiazole tethered 7-ethoxy quinoline hybrids: Synthesis and potential antimicrobial agents as dihydrofolate reductase (DHFR) inhibitors with molecular docking study. J. Mol. Struct. 1242, 130748. https://doi.org/https://doi.org/10.1016/j.molstruc.2021.130748.

Ammar, Y.A., Farag, A.A., Ali, A.M., Hessein, S.A., Askar, A.A., Fayed, E.A., Elsisi, D.M., Ragab, A., 2020a. Antimicrobial evaluation of thiadiazino and thiazolo quinoxaline hybrids as potential DNA gyrase inhibitors; design, synthesis, characterization and morphological studies. Bioorg. Chem. 99, 103841. https://doi.org/https://doi.org/10.1016/j.bioorg.2020.103841.

Ammar, Y.A., Farag, A.A., Ali, A.M., Ragab, A., Askar, A.A., Elsisi, D.M., Belal, A., 2020b. Design, synthesis, antimicrobial activity and molecular docking studies of some novel di-substituted sulfonylquinoxaline derivatives. Bioorg. Chem. 104, 104164. https://doi.org/https://doi.org/10.1016/j.bioorg.2020.104164.

Ammar, Y.A., Sh El-Sharief, A.M., Belal, A., Abbas, S.Y., Mohamed, Y.A., Mehany, A.B.M., Ragab, A., 2018. Design, synthesis, antiproliferative activity, molecular docking and cell cycle analysis of some novel (morpholinosulfonyl) isatins with potential EGFR inhibitory activity. Eur. J. Med. Chem. 156. https://doi.org/10.1016/j.ejmech.2018.06.061.

Ancizu, S., Moreno, E., Solano, B., Villar, R., Burguete, A., Torres, E., Pérez-Silanes, S., Aldana, I., Monge, A., 2010. New 3-methylquinoxaline-2-carboxamide 1, 4-di-N-oxide derivatives as anti-Mycobacterium tuberculosis agents. Bioorg. Med. Chem. 18, 2713–2719.

Ayliffe, G.A., 1997. The progressive intercontinental spread of methicillin-resistant Staphylococcus aureus. Clin. Infect. Dis. an Off. Publ. Infect. Dis. Soc. Am. 24 Suppl 1, S74–S79. https://doi.org/10.1093/clinids/24.supplement_1.s74.

Banerjee, P., Eckert, A.O., Schrey, A.K., Preissner, R., 2018. ProTox-II: a webserver for the prediction of toxicity of chemicals. Nucleic Acids Res. 46, W257–W263. https://doi.org/10.1093/nar/gky318.

Bough, R.G., Everest, R.P., Hale, L.J., Lessel, B., Mason, C.G., Spooner, D.F., 1971. Chemotherapeutic and Toxicological Properties of Quinacillin. Chemotherapy 16, 183–195. https://doi.org/10.1159/000220726.

Campoy, S., Adrio, J.L., 2017. Antifungals. Biochem. Pharmacol. 133, 86–96. https://doi.org/https://doi.org/10.1016/j.bcp.2016.11.019.

Cheesman, M.J., Ilanko, A., Blonk, B., Cock, I.E., 2017. Developing New Antimicrobial Therapies: Are Synergistic Combinations of Plant Extracts/Compounds with Conventional Antibiotics the Solution? Pharmacogn. Rev. 11, 57–72. https://doi.org/10.4103/phrev.phrev_21_17.

Christie, A.B., Mitchell, A.A.B., Walker, R.S., 1966. Quinacillin: A Study of a New Penicillin. Scott. Med. J. 11, 176–181. https://doi.org/10.1177/003693306601100505.

Collin, F., Karkare, S., Maxwell, A., 2011. Exploiting bacterial DNA gyrase as a drug target: current state and perspectives. Appl. Microbiol. Biotechnol. 92, 479–497. https://doi.org/10.1007/s00253-011-3557-z.

Daschner, F., 1977. Tetracyclines: bacteriostatic or bactericidal drugs? In vitro studies with rolitetracycline, minocycline and doxycycline (author's transl). Zentralbl. Bakteriol. Orig. A. 239, 527–534.

Denning, D.W., Bromley, M.J., 2015. How to bolster the antifungal pipeline. Science (80-.). 347, 1414 LP – 1416. https://doi.org/10.1126/science.aaa6097.

Denning, D.W., Hope, W.W., 2010. Therapy for fungal diseases: opportunities and priorities. Trends Microbiol. 18, 195–204. https://doi.org/https://doi.org/10.1016/j.tim.2010.02.004.

Dias, F.R.F., Novais, J.S., Devillart, T.A. do N.S., da Silva, W.A., Ferreira, M.O., Loureiro, R. de S., Campos, V.R., Ferreira, V.F., de Souza, M.C.B. V, Castro, H.C., Cunha, A.C., 2018. Synthesis and antimicrobial evaluation of amino sugar-based naphthoquinones and isoquinoline-5,8-diones and their halogenated compounds. Eur. J. Med. Chem. 156, 1–12. https://doi.org/https://doi.org/10.1016/j.ejmech.2018.06.050.

Eissa, S.I., Farrag, A.M., Abbas, S.Y., El Shehry, M.F., Ragab, A., Fayed, E.A., Ammar, Y.A., 2021. Novel Structural hybrids of quinoline and thiazole moieties: Synthesis and evaluation of antibacterial and antifungal activities with molecular modeling studies. Bioorg. Chem. 104803. https://doi.org/https://doi.org/10.1016/j.bioorg.2021.104803.

El-Attar, M.A.Z., Elbayaa, R.Y., Shaaban, O.G., Habib, N.S., Abdel Wahab, A.E., Abdelwahab, I.A., El-Hawash, S.A.M., 2018. Design, synthesis, antibacterial evaluation and molecular docking studies of some new quinoxaline derivatives targeting dihyropteroate synthase enzyme. Bioorg. Chem. 76, 437–448. https://doi.org/https://doi.org/10.1016/j.bioorg.2017.12.017.

El-Sabbagh, O.I., El-Sadek, M.E., Lashine, S.M., Yassin, S.H., El-Nabtity, S.M., 2009. Synthesis of new 2 (1H)-quinoxalinone derivatives for antimicrobial and antiinflammatory evaluation. Med. Chem. Res. 18, 782–797.

El-sharief, A.M.S., Ammar, Y.A., Belal, A., El-sharief, M.A.M.S., Mohamed, Y.A., Mehany, A.B.M., Elhag, G.A.M., Ragab, A., 2019. Design, synthesis, molecular docking and biological activity evaluation of some novel indole derivatives as potent anticancer active agents and apoptosis inducers. Bioorg. Chem. 85, 399–412. https://doi.org/10.1016/j.bioorg.2019.01.016.

El-Sharief, M.A.M.S., Abbas, S.Y., Zahran, M.A., Mohamed, Y.A., Ragab, A., Ammar, Y.A., 2016. New 1,3-diaryl-5-thioxo-imidazolidin-2,4-dione derivatives: Synthesis, reactions and evaluation of antibacterial and antifungal activities. Zeitschrift fur Naturforsch. - Sect. B. J. Chem. Sci. 71. https://doi.org/10.1515/znb-2016-0054.

Elsisi, D.M., Ragab, A., Elhenawy, A.A., Farag, A.A., Ali, A.M., Ammar, Y.A., 2022. Experimental and theoretical investigation for 6-Morpholinosulfonylquinoxalin-2(1H)-one and its haydrazone derivate: Synthesis, characterization, tautomerization and antimicrobial evaluation. J. Mol. Struct. 1247, 131314. https://doi.org/https://doi.org/10.1016/j.molstruc.2021.131314.

Epstein, M.E., Amodio-Groton, M., Sadick, N.S., 1997. Antimicrobial agents for the dermatologist. II. Macrolides, fluoroquinolones, rifamycins, tetracyclines, trimethoprim-sulfamethoxazole, and clindamycin. J. Am. Acad. Dermatol. 37, 365–384. https://doi.org/https://doi.org/10.1016/S0190-9622(97)70135-X.

Fayed, E.A., Ammar, Y.A., Ragab, A., Gohar, N.A., Mehany, A.B.M., Farrag, A.M., 2020. In vitro cytotoxic activity of thiazole-indenoquinoxaline hybrids as apoptotic agents, design, synthesis, physicochemical and pharmacokinetic studies. Bioorg. Chem. 100. https://doi.org/10.1016/j.bioorg.2020.103951.

Fayed, E.A., Ammar, Y.A., Saleh, M.A., Bayoumi, A.H., Belal, A., Mehany, A.B.M., Ragab, A., 2021a. Design, synthesis, antiproliferative evaluation, and molecular docking study of new quinoxaline derivatives as apoptotic inducers and EGFR inhibitors. J. Mol. Struct. 1236, 130317. https://doi.org/https://doi.org/10.1016/j.molstruc.2021.130317.

Fayed, E.A., Ragab, A., Ezz Eldin, R.R., Bayoumi, A.H., Ammar, Y. A., 2021b. In Vivo Screening and Toxicity Studies of Indolinone Incorporated Thiosemicarbazone, Thiazole and Piperidinosulfonyl Moieties as Anticonvulsant Agents. Bioorg. Chem. 105300. https://doi.org/https://doi.org/10.1016/j.bioorg.2021.105300.

Guillon, J., Mouray, E., Moreau, S., Mullié, C., Forfar, I., Desplat, V., Belisle-Fabre, S., Pinaud, N., Ravanello, F., Le-Naour, A., Léger, J.-M., Gosmann, G., Jarry, C., Déléris, G., Sonnet, P., Grellier, P., 2011. New ferrocenic pyrrolo[1,2-a]quinoxaline derivatives: Synthesis, and in vitro antimalarial activity – Part II. Eur. J. Med. Chem. 46, 2310–2326. https://doi.org/https://doi.org/10.1016/j.ejmech.2011.03.014.

Guo, J.-J., Dai, B.-L., Chen, N.-P., Jin, L.-X., Jiang, F.-S., Ding, Z.-S., Qian, C.-D., 2016. The anti-Staphylococcus aureus activity of the phenanthrene fraction from fibrous roots of Bletilla striata. BMC Complement. Altern. Med. 16, 491. https://doi.org/10.1186/s12906-016-1488-z.

Guo, M., Gao, Y., Xue, Y., Liu, Y., Zeng, X., Cheng, Y., Ma, J., Wang, H., Sun, J., Wang, Z., Yan, Y., 2021. Bacteriophage Cocktails Protect Dairy Cows Against Mastitis Caused By Drug Resistant Escherichia coli Infection. Front. Cell. Infect, Microbiol.

Hassan, A.S., Morsy, N.M., Awad, H.M., Ragab, A., 2021. Synthesis, molecular docking, and in silico ADME prediction of some fused pyrazolo[1,5-a]pyrimidine and pyrazole derivatives as potential antimicrobial agents. J. Iran. Chem. Soc. https://doi.org/10.1007/s13738-021-02319-4.

Ibrahim, S.A., Fayed, E.A., Rizk, H.F., Desouky, S.E., Ragab, A., 2021a. Hydrazonoyl bromide precursors as DHFR inhibitors for the synthesis of bis-thiazolyl pyrazole derivatives; antimicrobial activities, antibiofilm, and drug combination studies against MRSA. Bioorg. Chem. 105339. https://doi.org/https://doi.org/10.1016/j.bioorg.2021.105339.

Ibrahim, S.A., Rizk, H.F., Aboul-Magd, D.S., Ragab, A., 2021b. Design, synthesis of new magenta dyestuffs based on thiazole azomethine disperse reactive dyes with antibacterial potential on both dyes and gamma-irradiated dyed fabric. Dye. Pigment. 193, 109504. https://doi.org/https://doi.org/10.1016/j.dyepig.2021.109504.

Ito, A., Budke, C.M., 2021. Genetic Diversity of Taenia solium and its Relation to Clinical Presentation of Cysticercosis. Yale J. Biol. Med. 94, 343–349.

Khan, S.A., Asiri, A.M., 2011. Synthesis of novel steroidal oxazolo quinoxaline as antibacterial agents. Arab. J. Chem. 4, 349–354. https://doi.org/https://doi.org/10.1016/j.arabjc.2010.06.058.

Khan, S.A., Mullick, P., Pandit, S., Kaushik, D., 2009. Synthesis of hydrazones derivatives of quinoxalinone-prospective antimicrobial and antiinflammatory agents. Acta Pol. Pharm. 66, 169–172.

Khatoon, H., Abdulmalek, E., 2021. Novel Synthetic Routes to Prepare Biologically Active Quinoxalines and Their Derivatives: A Synthetic Review for the Last Two Decades. Mol. https://doi.org/10.3390/molecules26041055.

Kim, Y.B., Kim, Y.H., Park, J.Y., Kim, S.K., 2004. Synthesis and biological activity of new quinoxaline antibiotics of echinomycin analogues. Bioorg. Med. Chem. Lett. 14, 541–544. https://doi.org/https://doi.org/10.1016/j.bmcl.2003.09.086.

Kusakabe, Y., Mizutani, S., Kamo, S., Yoshimoto, T., Tomoshige, S., Kawasaki, T., Takasawa, R., Tsubaki, K., Kuramochi, K., 2019. Synthesis, antibacterial and cytotoxic evaluation of flavipucine and its derivatives. Bioorg. Med. Chem. Lett. 29, 1390–1394. https://doi.org/https://doi.org/10.1016/j.bmcl.2019.03.034.

Langebrake, C., Rohde, H., Lellek, H., Wolschke, C., Kröger, N.M., 2014. Micafungin as antifungal prophylaxis in recipients of allogeneic hematopoietic stem cell transplantation: results of different dosage levels in clinical practice. Clin. Transplant. 28, 286–291. https://doi.org/https://doi.org/10.1111/ctr.12310.

Liu, X., Ling, Z., Li, L., Ruan, B., 2011. Invasive fungal infections in liver transplantation. Int. J. Infect. Dis. 15, e298–e304. https://doi.org/https://doi.org/10.1016/j.ijid.2011.01.005.

Matson, J.B., Stupp, S.I., 2011. Drug release from hydrazone-containing peptide amphiphiles. Chem. Commun. 47, 7962–7964.

Mitevska, E., Wong, B., Surewaard, B.G.J., Jenne, C.N., 2021. The Prevalence, Risk, and Management of Methicillin-Resistant Staphylococcus aureus Infection in Diverse Populations across Canada: A Systematic Review. Pathog. https://doi.org/10.3390/pathogens10040393.

Miyagawa, M., 2010. Globally harmonized system of classification and labelling of chemicals (GHS) and its implementation in Japan. Nihon Eiseigaku Zasshi. 65, 5–13. https://doi.org/10.1265/jjh.65.5.

Mondal, S., Mandal, S.M., Mondal, T.K., Sinha, C., 2017. Spectroscopic characterization, antimicrobial activity, DFT computation and docking studies of sulfonamide Schiff bases. J. Mol. Struct. 1127, 557–567. https://doi.org/https://doi.org/10.1016/j.molstruc.2016.08.011.

Muhammad, Z.A., Edrees, M.M., Faty, R.A.M., Gomha, S.M., Alterary, S.S., Mabkhot, Y.N., 2017. Synthesis, Antitumor Evaluation and Molecular Docking of New Morpholine Based Heterocycles. Mol. . https://doi.org/10.3390/molecules22071211.

Özbek, N., Katırcıoğlu, H., Karacan, N., Baykal, T., 2007. Synthesis, characterization and antimicrobial activity of new aliphatic sulfonamide. Bioorg. Med. Chem. 15, 5105–5109. https://doi.org/https://doi.org/10.1016/j.bmc.2007.05.037.

R.L. Baehner, D.G.N., 1968. Quantitative nitroblue tetrazolium test in chronic granulomatous disease. N. Engl. J. Med. 278, 971–976.

Ragab, A., Fouad, S.A., Ali, O.A.A., Ahmed, E.M., Ali, A.M., Askar, A.A., Ammar, Y.A., 2021. Sulfaguanidine Hybrid with Some New Pyridine-2-One Derivatives: Design, Synthesis, and Antimicrobial Activity against Multidrug-Resistant Bacteria as Dual DNA Gyrase and DHFR Inhibitors. Antibiotics 10, 162. https://doi.org/10.3390/antibiotics10020162.

Ragavendran, J.V., Sriram, D., Patel, S.K., Reddy, I.V., Bharathwajan, N., Stables, J., Yogeeswari, P., 2007. Design and synthesis of anticonvulsants from a combined phthalimide–GABA–anilide and hydrazone pharmacophore. Eur. J. Med. Chem. 42, 146–151. https://doi.org/https://doi.org/10.1016/j.ejmech.2006.08.010.

Rahman, V.P.M., Mukhtar, S., Ansari, W.H., Lemiere, G., 2005. Synthesis, stereochemistry and biological activity of some novel long alkyl chain substituted thiazolidin-4-ones and thiazan-4-one from 10-undecenoic acid hydrazide. Eur. J. Med. Chem. 40, 173–184. https://doi.org/https://doi.org/10.1016/j.ejmech.2004.10.003.

Rizk, H.F., El Borai, M.A., Ragab, A., Ibrahim, S.A., 2020. Design, synthesis, biological evaluation and molecular docking study based on novel fused pyrazolothiazole scaffold. J. Iran. Chem. Soc. 17, 2493–2505. https://doi.org/DOI 10.1007/s13738-020-01944-9.

Sakata, G., Makino, K., Kurasawa, Y., 1988. Regent progress in the quinoxaline chemistry. Synthesis and biological activity. Heterocycles (Sendai) 27, 2481–2515.

Salem, M.A., Ragab, A., Askar, A.A., El-Khalafawy, A., Makhlouf, A.H., 2020a. One-pot synthesis and molecular docking of some new spiropyranindol-2-one derivatives as immunomodulatory agents and in vitro antimicrobial potential with DNA gyrase inhibitor. Eur. J. Med. Chem. 188. https://doi.org/10.1016/j.ejmech.2019.111977.

Salem, M.A., Ragab, A., El-Khalafawy, A., Makhlouf, A.H., Askar, A.A., Ammar, Y.A., 2020b. Design, synthesis, in vitro antimicrobial evaluation and molecular docking studies of indol-2-one tagged with morpholinosulfonyl moiety as DNA gyrase inhibitors. Bioorg. Chem. 96. https://doi.org/10.1016/j.bioorg.2020.103619.

Salgın-Gökşen, U., Gökhan-Kelekçi, N., Göktaş, Ö., Köysal, Y., Kılıç, E., Işık, Ş., Aktay, G., Özalp, M., 2007. 1-Acylthiosemicarbazides, 1,2,4-triazole-5(4H)-thiones, 1,3,4-thiadiazoles and hydrazones containing 5-methyl-2-benzoxazolinones: Synthesis, analgesic-anti-inflammatory and antimicrobial activities. Bioorg. Med. Chem. 15, 5738–5751. https://doi.org/https://doi.org/10.1016/j.bmc.2007.06.006.

Salwan, R., Sharma, V., 2020. Chapter 15 - Bioactive compounds of Streptomyces: Biosynthesis to applications, in: Atta-Ur-Rahman,

B.T.-S. in N.P.C. (Ed.), Bioactive Natural Products. Elsevier, pp. 467–491. https://doi.org/https://doi.org/10.1016/B978-0-12-817903-1.00015-2.

Sanna, P., Carta, A., Loriga, M., Zanetti, S., Sechi, L., 1998. Synthesis of substituted 2-ethoxycarbonyl- and 2-carboxyquinoxalin-3-ones for evaluation of antimicrobial and anticancer activity. Farm. 53, 455–461. https://doi.org/https://doi.org/10.1016/S0014-827X(98)00044-5.

Sarges, R., Howard, H.R., Browne, R.G., Lebel, L.A., Seymour, P.A., Koe, B.K., 1990. 4-Amino [1, 2, 4] triazolo [4, 3-a] quinoxalines. A novel class of potent adenosine receptor antagonists and potential rapid-onset antidepressants. J. Med. Chem. 33, 2240–2254.

Selim, M.R., Zahran, M.A., Belal, A., Abusaif, M.S., Shedid, S.A., Mehany, A., Elhagali, G.A.M., Ammar, Y.A., 2019. Hybridized Quinoline Derivatives as Anticancer Agents: Design, Synthesis, Biological Evaluation and Molecular Docking. Anti-Cancer Agents Med. Chem. (Formerly Curr. Med. Chem. Agents) 19, 439–452.

Shōji, J.-I., Katagiri, K., 1961. Studies on Quinoxaline Antibiotics. III New Antibiotics, Triostins A, B and C. J. Antibiot. Ser. A 14, 335–339. https://doi.org/10.11554/antibioticsa.14.6_335.

Smilack, J.D., 1999. Trimethoprim-Sulfamethoxazole. Mayo Clin. Proc. 74, 730–734. https://doi.org/https://doi.org/10.4065/74.7.730.

Sun, N., Li, M., Cai, S., Li, Y., Chen, C., Zheng, Y., Li, X., Fang, Z., Lv, H., Lu, Y.-J., 2019. Antibacterial evaluation and mode of action study of BIMQ, a novel bacterial cell division inhibitor. Biochem. Biophys. Res. Commun. 514, 1224–1230.

Surarit, R., Shepherd, M.G., 1987. The effects of azole and polyene antifungals on the plasma membrane enzymes of Candida albicans. J. Med. Vet. Mycol. 25, 403–413. https://doi.org/10.1080/02681218780000491.

Ughetto, G., Wang, A.H., Quigley, G.J., van der Marel, G.A., van Boom, J.H., Rich, A., 1985. A comparison of the structure of echinomycin and triostin A complexed to a DNA fragment. Nucleic Acids Res. 13, 2305–2323. https://doi.org/10.1093/nar/13.7.2305.

Verma, G., Marella, A., Shaquiquzzaman, M., Akhtar, M., Ali, M.R., Alam, M.M., 2014. A review exploring biological activities of hydrazones. J. Pharm. Bioallied Sci. 6, 69–80. https://doi.org/10.4103/0975-7406.129170.

Wanger, A., Chávez, V., 2021. Antibiotic susceptibility testing. Practical Handbook of Microbiology. CRC Press, 119–128.

Wassel, M.M.S., Ammar, Y.A., Elhag Ali, G.A.M., Belal, A., Mehany, A.B.M., Ragab, A., 2021a. Development of adamantane scaffold containing 1,3,4-thiadiazole derivatives: Design, synthesis, anti-proliferative activity and molecular docking study targeting EGFR. Bioorg. Chem. 110, 104794. https://doi.org/https://doi.org/10.1016/j.bioorg.2021.104794.

Wassel, M.M.S., Ragab, A., Elhag Ali, G.A.M., Mehany, A.B.M., Ammar, Y.A., 2021b. Novel adamantane-pyrazole and hydrazone hybridized: Design, synthesis, cytotoxic evaluation, SAR study and molecular docking simulation as carbonic anhydrase inhibitors. J. Mol. Struct. 1223, 128966. https://doi.org/https://doi.org/10.1016/j.molstruc.2020.128966.

Wikler, M.A., Hindler, J.F., Cockerill, F.R., Patel, J.B., Bush, K., Powell, M., Dudley, M.N., Turnidge, J.D., Elopoulos, G.M. and Weinstein, M.P., 2008. Clinical and Laboratory Standards Institute, in: Methods for Dilution Antimicrobial Susceptibility Tests for Bacteria That Grow Aerobically; Approved Standard, ; CLSI Document M07-A8; ISBN: ISBN 1-56238-689-1. Wayne, PA, USA.

Wise, R., Hart, T., Cars, O., Streulens, M., Helmuth, R., Huovinen, P., Sprenger, M., 1998. Antimicrobial resistance. Is a major threat to public health. BMJ 317, 609–610. https://doi.org/10.1136/bmj.317.7159.609.

Xu, F., Cheng, G., Hao, H., Wang, Y., Wang, X., Chen, D., Peng, D., Liu, Z., Yuan, Z., Dai, M., 2016. Mechanisms of Antibacterial Action of Quinoxaline 1,4-di-N-oxides against Clostridium perfringens and Brachyspira hyodysenteriae. Front. Microbiol. 7, 1948. https://doi.org/10.3389/fmicb.2016.01948.

Yang, Y., Zhang, S., Wu, B., Ma, M., Chen, X., Qin, X., He, M., Hussain, S., Jing, C., Ma, B., 2012. An efficient synthesis of quinoxalinone derivatives as potent inhibitors of aldose reductase. ChemMedChem 7, 823–835.

Z El-Attar, M.A., Elbayaa, R.Y., Shaaban, O.G., Habib, N.S., Abdel Wahab, A.E., Abdelwahab, I.A., M El-Hawash, S.A., 2018. Synthesis of pyrazolo-1,2,4-triazolo[4,3-a]quinoxalines as antimicrobial agents with potential inhibition of DHPS enzyme. Future Med. Chem. 10, 2155–2175. https://doi.org/10.4155/fmc-2018-0082.

Zhao, S., Wei, P., Wu, M., Zhang, X., Zhao, L., Jiang, X., Hao, C., Su, X., Zhao, D., Cheng, M., 2018. Design, synthesis and evaluation of benzoheterocycle analogues as potent antifungal agents targeting CYP51. Bioorg. Med. Chem. 26, 3242–3253. https://doi.org/https://doi.org/10.1016/j.bmc.2018.04.054.